

This is a non-peer reviewed pre-print submitted to EarthArxiv.
Subsequent peer-reviewed versions of this manuscript may have slightly different content. The authors welcome feedback.

Please contact Sandy H. S. Herho (sandy.herho@email.ucr.edu) regarding this manuscript's content.

imc-precip-iso: Open monthly stable isotope data of precipitation over the Indonesian Maritime Continent

R. Suwarman¹, S. H. S. Herho^{2,3,*}, H. A. Belgaman⁴, D. E. Irawan⁵, K. Ichiyanagi⁶, I. M. Yosa¹, A. I. D. Utami⁷, S. Prayogo⁸, and E. Aldrian⁴

¹Atmospheric Science Research Group, Bandung Institute of Technology (ITB), Bandung, Indonesia

²Department of Earth and Planetary Sciences, University of California, Riverside, USA

³Department of Geology, University of Maryland, College Park, USA

⁴Research Center for Climate and Atmosphere (PRIMA), National Research and Innovation Agency (BRIN), Bandung, Indonesia

⁵Applied Geology Research Group, Bandung Institute of Technology (ITB), Bandung, Indonesia

⁶Faculty of Advanced Science and Technology, Kumamoto University, Kumamoto, Japan

⁷Indonesian Meteorology, Climatology, and Geophysical Agency (BMKG), Jakarta, Indonesia

⁸Software Engineering Division, Manvis Teknologi Engineering, Bandung, Indonesia

*Corresponding author: sandy.herho@email.ucr.edu

Abstract

Stable isotopes, $\delta^2\text{H}$, $\delta^{18}\text{O}$, and d-excess, are valuable tools as natural tracers of diffusion processes and phase changes in the global hydroclimatological cycle. The Indonesian Maritime Continent (IMC) is an archipelago area surrounded by very warm waters which induce convective activities as the primary heat source driving global atmospheric circulation. Given the central role of IMC in this hydroclimatological cycle, comprehensive study and data collection on the stable isotopes of precipitation in this region is crucial.

In this study, we collected monthly stable isotope data from 62 stations spread throughout the Indonesian archipelago from September 2010 to September 2017. We cleaned the data and conducted quality control activities by comparing the Local Meteoric Water Line (LMWL) to previous studies in a similar climatic region. We shared these data openly on our GitHub repository, making them easier to update and interact with users in the future.

1 Introduction

Indonesian Maritime Continent (IMC) comprises a group of islands surrounded by the Indian and Pacific Oceans. The region's climate is influenced by its insular geography and its position near the Equator. Located in the western part of the Indo-Pacific warm pool (IPWP), IMC is a source of latent heat release and deep convection which drives the Hadley and Walker cells, thus playing an essential role in the earth's hydrological cycle (1; 2). IMC is also the only link for warmed surface waters from the Pacific Ocean to the Indian Ocean through the Indonesian Throughflow (ITF), a surface flow component of the global ocean conveyor belt (e. g. 3; 4; 5; 6; 7).

In general, IMC experiences two seasons, namely the wet and dry seasons, each in boreal winter - spring (November-March/NDJFM) and boreal summer - fall (May - September/MJJAS) (8; 1). During the wet season, there is warm sea surface temperature (SST) and heavy precipitation over the IMC, which is brought by the Asian winter monsoon, which is northeasterly to the north of the equator and northwesterly to the south of the equator, the opposite also happens in the dry season (9; 10; 1). Besides the annual cycle, IMC precipitation is influenced by internal global atmosphere-ocean interactions, such as the El Niño Southern Oscillation (ENSO) (e. g. 11; 12; 13; 14; 15) and the Indian Ocean Dipole mode (IOD) (e. g. 1; 16; 11; 17). On an

45 intra-annual scale, precipitation over the IMC is also influenced by the Madden-Julian Oscillation (MJO),
46 which propagates from the Indian Ocean to the Pacific Ocean via IMC (e. g. 18; 19; 11; 20; 21; 22).

47 Given the importance of IMC in understanding the earth's hydroclimatological phenomena (23), investiga-
48 tion of precipitation characteristics is inevitable. One of the characteristics of precipitation that is important
49 to investigate is the traditional water-stable isotopes of precipitation ($\delta^{18}\text{O}$ and $\delta^2\text{H}$) which are considered
50 one of the natural tracers of hydrological cycles as a consequence of equilibrium and kinetic processes dur-
51 ing phase transitions and diffusive processes (24; 25; 26; 27). In general, oxygen-18 ($\delta^{18}\text{O}$) and deuterium
52 ($\delta^2\text{H}$) at mid- and high-latitudes are correlated with temperature (e. g. 28; 29; 30; 31; 32). However, in tropi-
53 cal regions such as the IMC, these two isotopic compositions show a negative correlation (e.g. 33; 34; 35; 36)
54 due to a rainout process known as the amount effect (37). $\delta^{18}\text{O}$ can also be used as a signature of the wa-
55 ter vapour transport process during ENSO and MJO over the IMC (38; 39; 40). Observations of $\delta^{18}\text{O}$ and
56 $\delta^2\text{H}$ in the tropics are also crucial to confirm the sensitivity of proxy precipitation observations in paleo-
57 climatology using proxy system modelling (PSM), which requires modern precipitation isotope data in the
58 region (41). Modern precipitation isotope observations are also needed to correct calculations performed
59 by isotope-enabled General Circulation Models (iGCMs) (e. g. 42; 43; 44; 45).

60 Until recently, there is not much open and publicly accessible data on traditional precipitation isotope
61 over the IMC. There are four isotope stations operated by the International Atomic Energy Agency (IAEA)
62 within the framework of the Global Network of Isotopes in Precipitation (GNIP) program. However, these
63 stations stopped operating in 2003 and only cover the Java region, except for the Jayapura station in Papua
64 (46). In addition, there were isotope observations conducted by the Institute of Observational Research
65 for Global Change (IORGC)/Japan Agency for Marine-Earth Science and Technology (JAMSTEC) conducted
66 at six stations across IMC between 2001 and 2007 (33; 46).

67 In this study, we conducted monthly $\delta^{18}\text{O}$ and $\delta^2\text{H}$ sampling at 62 observation stations along the IMC
68 from September 2010 to September 2017. Part of these data (30 stations) have been used in a study by
69 Belgaman et al. (47) but has yet to be opened to the public. We opened the $\delta^{18}\text{O}$ and $\delta^2\text{H}$ measurements
70 to the public on our GitHub repository to support democratizing knowledge based on open-source code
71 and reproducible datasets (48).

72 2 Material and Methods

73 2.1 Data Acquisition

74 We conducted field sampling from 62 meteorological and climatological stations owned by the Indonesian
75 Meteorology, Climatology, and Geophysical Agency (BMKG) throughout the IMC area (Figure 1). To find out
76 the details of station numbering and their location, see the table on the following URL: https://github.com/sandyherho/imc-precip-iso/blob/main/output_data/sta_list.csv. We collected these pre-
77 cipitation samples manually using buckets and then put them into 6 mL glass vials with screw caps. We
78 collected this monthly precipitation samples from September 2010 to September 2017.

80 We measured $\delta^{18}\text{O}$ and $\delta^2\text{H}$ using the Picarro[®] L2120-i instrument using the cavity ring-down spectroscopy
81 technique, which has proven practical and accurate in measuring water isotopes (e. g. 51; 52; 53; 54; 55).
82 We measured the ratio of the abundance of the heavy to light isotopes (R), in the context of this study,
83 $^2\text{H}/^1\text{H}$ and $^{18}\text{O}/^{16}\text{O}$, from samples by comparing them to the international standard, namely the Vienna
84 Standard Mean Ocean Water (VSMOW) (56) so that δ values were obtained in units per mil (‰) using the
85 following equation:

$$\delta = \left(\frac{R_{\text{sample}}}{R_{\text{standard}}} - 1 \right) \times 10^3 \quad (1)$$

86 Due to the limited supply of international standards (is), we calibrated the samples (x) using three working
87 standards (ws), Aqua Standard[®], SLW2 and ICE2, which had been calibrated against VSMOW. This calcula-
88 tion process is formulated through the following equation (57):

$$\delta_{x-is} = \delta_{x-ws} + \delta_{ws-is} + (\delta_{x-ws} \times \delta_{ws-is}) \times 10^{-3} \quad (2)$$

89 Long-term standard errors (1σ) for these $\delta^{18}\text{O}$ and $\delta^2\text{H}$ measurements are ± 0.08 ‰ and ± 0.22 ‰, re-
90 spectively (47).

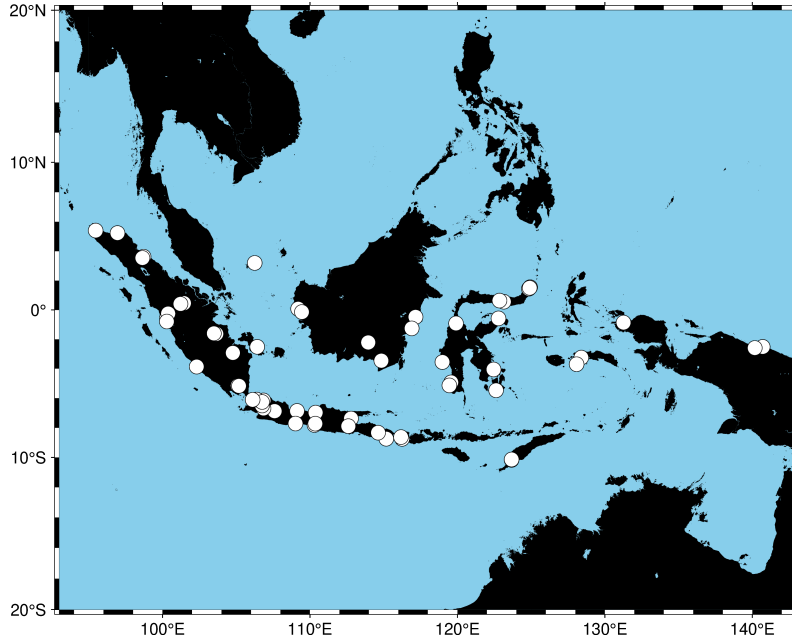


Figure 1: Location of the stations at which monthly samples of precipitation were collected for isotope measurements over the IMC (rendered using PyGMT (49; 50)).

2.2 Data Wrangling

Microsoft® Excel files extracted from the isotope measurement instrument were then converted into a text-formatted files, i. e. comma-separated values (CSV) format to make them easier to read by various kinds of software without being limited by a paid license (58; 59). These data were then splitted into time series for each station and the entire IMC. In addition, we also calculated d-excess (d), which is defined as the deviation from $\delta^2\text{H}$ to $\delta^{18}\text{O}$ according to the definition of the Global Meteoric Water Line (GMWL) (60), which can be written as follows:

$$d = \delta^2\text{H} - 8\delta^{18}\text{O} \quad (3)$$

Calculation of this d-excess is necessary, given its correlation with the oceanic source of precipitation (61; 28). Globally, this d-excess is a dependent variable of the relative humidity of the sea surface (62). Using d-excess, we can find the moisture flux anomaly during extreme events, such as ENSO influences in precipitation (e. g. 63; 64; 65). We did the entire data wrangling process using NumPy (66) and pandas (67) libraries in the Python computing environment.

2.3 Local Meteoric Water Line (LMWL) Estimation

We performed Local Meteoric Water Line (LMWL) calculations as part of our quality control efforts. It has been known since a study conducted by Craig (60) that there is a linear relationship between $\delta^2\text{H}$ to $\delta^{18}\text{O}$ globally, which can be formulated as follows:

$$\delta^2\text{H} = 8\delta^{18}\text{O} + 10 \quad (4)$$

However, local slope variations and intercepts were only discovered after collecting IAEA/GNIP observations through the study of Rozanski et al. (68), better known as LMWL. In this study, it is emphasized that the relationship between the two isotopes is still linear. Variations in the slope may store information about the local seasonal climatology (69).

We used Bayesian Linear Regression (BLR) to determine the relationship between $\delta^2\text{H}$ and $\delta^{18}\text{O}$ over the IMC. BLR allows better handling of uncertainty in models. This method recognizes that we need perfect information about model parameters or data variability. We can represent this uncertainty using a probability distribution on the parameters in the Bayesian approach. This approach helps generate more realistic and credible parameter estimates and confidence intervals. The BLR approach allows us to incorporate any

116 prior knowledge about the model parameters. This is useful when we need more data or want to use ex-
 117 isting domain knowledge. In this study, we determined the priors for slopes and intercepts from the global
 118 data compilation for humid tropical regions (Köppen class A) that was done by Putman et al. (69). Apart
 119 from single-point estimates (as in "frequentist" linear regression), the BLR gives a full posterior distribu-
 120 tion of model parameters after looking at the data. This provides richer information about the parameter
 121 uncertainties and allows for more robust modelling of the $\delta^2\text{H} - \delta^{18}\text{O}$ covariance. Because of these ad-
 122 vantages, the Bayesian approaches have recently been popular for solving water isotope problems (e. g.
 123 69; 70; 71; 72; 73; 74; 75). The full benefits of using BLR can be found in Klauenberg et al. (76).

124 The simple linear regression model that we used to explain the statistical relationship between $\delta^2\text{H}$ and
 125 $\delta^{18}\text{O}$ is illustrated in the following equation:

$$\delta^2\text{H}_i = \beta_0 + \beta_1\delta^{18}\text{O}_i + \varepsilon_i \quad (5)$$

126 , where $\delta^2\text{H}_i$ and $\delta^{18}\text{O}_i$ are the observed deuterium and oxygen-18 isotope values for the i -th data point,
 127 respectively. β_0 and β_1 are the unknown regression coefficients (intercept and slope) to be estimated.
 128 ε_i is the random error term, assumed to be normally distributed, with mean zero and constant variance
 129 σ^2 .

130 BLR estimation started by specifying the prior distributions for the unknown parameters: β_0 , β_1 , and σ^2 .
 131 In this study, we assumed normal prior for intercept and slope, and uniform prior for variance (77):

$$\begin{cases} \beta_0 \sim \mathcal{N}(m_0, s_0^2) \\ \beta_1 \sim \mathcal{N}(m_1, s_1^2) \\ \sigma^2 \sim U(a, b) \end{cases} \quad (6)$$

132 Parameters m_0 , m_1 , s_0 , s_1 , a , and b were determined from the global observation database for the humid
 133 tropical regions (Köppen class A) (69).

134 Assuming errors ε_i are normally distributed, the likelihood function can be written in the following form:

$$p(\delta^2\text{H}_i | \beta_0, \beta_1, \delta^{18}\text{O}_i, \sigma^2) = \frac{1}{\sqrt{2\pi\sigma^2}} \exp\left(-\frac{(\delta^2\text{H}_i - \beta_0 - \beta_1\delta^{18}\text{O}_i)^2}{2\sigma^2}\right) \quad (7)$$

135 The joint posterior distribution of the BLR parameters given the observed isotope data ($\delta^2\text{H}_i, \delta^{18}\text{O}_i$) is:

$$p(\beta_0, \beta_1, \sigma^2 | \text{data}) \propto p(\text{data} | \beta_0, \beta_1, \sigma^2) \times p(\beta_0) \times p(\beta_1) \times p(\sigma^2) \quad (8)$$

136 , where $p(\text{data} | \beta_0, \beta_1, \sigma^2)$ is the likelihood and $p(\beta_0)$, $p(\beta_1)$, and $p(\sigma^2)$ are the priors.

138 We used a simple algorithm from the Markov chain Monte Carlo (MCMC) methods (78), the Metropolis-
 139 Hastings (MH) algorithm (79; 80), to estimate the posterior distribution. This algorithm can approximate
 140 the posterior distribution without the need to compute the normalization constant (81). MH algorithm has
 141 also proven reliable enough to be used in hydroclimatological problems (e. g. 69; 82; 83; 84; 85; 86; 87; 88).
 142 MH algorithm can be summarized into several steps as follows:

- 143 1. Initialize the parameters $\beta_0^{(0)}$, $\beta_1^{(0)}$, and $\sigma_0^{2(0)}$ to some initial values.
- 144 2. For iteration $t = 1$ to T , where T is the number of iterations (in this study, we used 10,000 steps
 145 with the tuning of 2,000 steps which are the "burn in" iterations used to accelerate convergence
 146 (78; 89)):

- 147 (a) Calculate the acceptance ratio α :

$$\alpha = \frac{p(\text{data} | \beta_0, \beta_1, \sigma^{2*}) \times p(\beta_0) \times p(\beta_1) \times p(\sigma^{2*})}{p(\text{data} | \beta_0^{(t-1)}, \beta_1^{(t-1)}, \sigma^{2(t-1)}) \times p(\beta_0^{(t-1)}) \times p(\beta_1^{(t-1)}) \times p(\sigma^{2(t-1)})} \quad (9)$$

- 148 (b) Generate a uniform random number u from $[0, 1]$.

- 149 (c) If $u < \alpha$, accept the proposed parameters: $\beta_0^{(t)} = \beta_0, \beta_1^{(t)} = \beta_1, \sigma^{2(t)} = \sigma^{2*}$. Otherwise,
 150 keep the previous parameters: $\beta_0^{(t)} = \beta_0^{(t-1)}, \beta_1^{(t)} = \beta_1^{(t-1)}, \sigma^{2(t)} = \sigma^{2(t-1)}$.

151 3. After T iterations, we have samples from the posterior distribution. We use these samples to esti-
 152 mate the posterior mean, credible intervals, and other properties of the parameters.

153 This study uses a symmetrical Gaussian proposal distribution to simplify computing the acceptance ratio
 154 (78; 90; 89; 91). We implemented the entire BLR process using the **PyMC3** library within the Python com-
 155 puting environment (92).

156 3 Results and Discussion

157 The number of data points at each isotope observation station can be seen in Figure 2. The three stations
 158 with the most data collection were the Kemayoran Air Pollution Post in Jakarta (#1), with a total of 47 data
 159 points, followed by Deli Serdang in North Sumatra (#5) with a total of 46 data points, and in third place is the
 160 Bengkulu station (#11) which is located on the southwest coast of Sumatra with a total of 43 observations of
 161 data points. The stations with the fewest number of observations include Tambang (#57), located in Riau,
 162 and Ranomeeto (#58) in Southeast Sulawesi, each with two data points. Stations with the second-fewest
 163 number of observations include El Tari (#24) and Kupang in East Nusa Tenggara (#38), Mlati (#49) in Sleman,
 164 Yogyakarta, Malikusaleh (#53) in North Aceh, Koba (#56) in Bangka Belitung, each of which recorded only
 165 three data points. The stations with the third-fewest number of observations are Tarempa (#36) in the Riau
 166 Archipelago, West Seram (#48) in Maluku, and Sorong (#54) in Southwest Papua, each of which only has
 167 four data points. All stations' average and median data points were 21.968 and 22, respectively. These are
 168 very small because only about a quarter of the 85 months of observation period had successfully extracted
 169 $\delta^2\text{H}$ and $\delta^{18}\text{O}$ values.

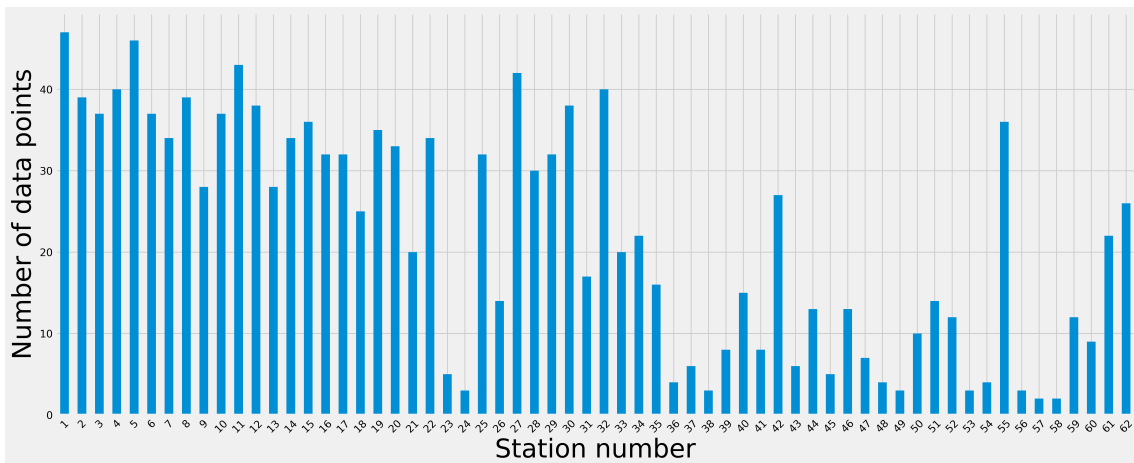


Figure 2: Availability of data points at each isotope station over the IMC collected in this study.

170 Weaknesses in data collection are also found in the need for more coverage of areas outside parts of Suma-
 171 tra and Java due to limited access to transportation for sending samples. This must be underlined because
 172 most of the isotope measurements we produced in this study are concentrated in a region with monsoonal
 173 rainfall classifications (8; 93; 94). In contrast, anti-monsoonal and semi-annual regions are underrepre-
 174 sented. This is also evident in the less distribution of $\delta^2\text{H}$ and $\delta^{18}\text{O}$ values at stations in these two regions,
 175 as shown in the boxplots in Figure 3.

176 By combining $\delta^2\text{H}$ and $\delta^{18}\text{O}$ from all stations, we performed BLR inference, where the results of trace
 177 plots and the posterior distribution of the linear regression parameters can be seen in Figure 4. There is a
 178 convergence of all linear regression parameters, which can be visually seen in the trace plots (Figure 4a).
 179 The posterior distribution of the LMWL parameters that have been calculated using the MH algorithm is
 180 shown in Figure 4b. The mean and standard deviation of the posterior intercept are 3.506 ‰ and 1.732 ‰,
 181 respectively. Meanwhile, the mean and standard deviation of the posterior slope are 7.298 ‰ and 0.267
 182 ‰, respectively. Then, for a 2σ credible interval, we can write the LMWL equation as follows:

$$\delta^2\text{H} = 7.298(\pm 0.534)\delta^{18}\text{O} + 3.506(\pm 3.464) \quad (10)$$

183 The two regression coefficients in Equation 10 are shallower when compared to GMWL. This indicates

184 the occurrence of a sub-cloud evaporation process which indicates the occurrence of re-evaporation from
185 rainwater after falling under the clouds through a tropical convective processes. Visually this can be seen
186 by shifting the LMWL regression line clockwise when compared to the GMWL (Figure 5). Similar things
187 were also found in previous studies over the Maritime Continent (95; 96; 26).

188 4 Conclusion

189 Based on water isotope observations from 62 stations that we collected from September 2010 to Septem-
190 ber 2017, we managed to build monthly $\delta^2\text{H}$, $\delta^{18}\text{O}$, and d-excess datasets per station and for all IMC, which
191 are shared openly, accessible, and easily updated on the GitHub repository. We have also performed quality
192 control on these data by calculating the LMWL using BLR, which is under the range of slopes and intercepts
193 in previous studies conducted in areas with similar climate types (e. g. 95; 96; 69; 26). The open data we
194 shared are by far the most complete data over the IMC for stable isotopes of precipitation.

195 There are limitations to this study. One of them is that we should have checked the amount effect. This is
196 due to the limitation of station precipitation data, which contains many empty data. In the future, a combi-
197 nation of station data and other high-resolution data sources is needed, such as the Climate Hazards Group
198 InfraRed Precipitation with Station data (CHIRPS) (97), which can be used to calculate the amount effect.
199 In addition, this monthly water isotope observation activities over the IMC were stopped in September
200 2017. This activity should be continued, given the central position of the IMC in the Earth's climate sys-
201 tem, which is currently undergoing significant changes as a consequence of the unprecedented increase
202 in anthropogenic radiative forcing. The study of water isotopes in precipitation over the IMC can undoubt-
203 edly deepen our understanding of anthropogenic and natural attributions in the hydrologic cycle in the
204 tropics.

205 Acknowledgments

206 We are grateful to Michael N. Evans (UMD) for discussing fractionation on precipitation isotopes in the
207 tropics, which was useful in producing these data. This study was supported by ITB Research, Community
208 Service and Innovation Program (PPMI-ITB) and Japan Society for the Promotion of Science (JSPS) KAKENHI
209 (#24510256 and #16H05619). Open-source code and publicly available data can be accessed from: <https://github.com/sandyherho/imc-precip-iso/>.
210

211 References

- 212 [1] S. Yang, T. Zhang, Z. Li, and S. Dong, "Climate variability over the maritime continent and its role in
213 global climate variation: A review," *Journal of Meteorological Research*, vol. 33, no. 6, pp. 993–1015,
214 2019.
- 215 [2] P. Xue, P. Malanotte-Rizzoli, J. Wei, and E. A. B. Eltahir, "Coupled ocean-atmosphere modeling
216 over the Maritime Continent: A review," *Journal of Geophysical Research: Oceans*, vol. 125, no. 6,
217 p. e2019JC014978, 2020.
- 218 [3] J. S. Godfrey, "The effect of the Indonesian throughflow on ocean circulation and heat exchange with
219 the atmosphere: A review," *Journal of Geophysical Research: Oceans*, vol. 101, no. C5, pp. 12217–12237,
220 1996.
- 221 [4] M. Li, A. L. Gordon, L. K. Gruenburg, J. Wei, and S. Yang, "Interannual to decadal response of the
222 Indonesian throughflow vertical profile to Indo-Pacific forcing," *Geophysical Research Letters*, vol. 47,
223 no. 11, p. e2020GL087679, 2020.
- 224 [5] S. Makarim, J. Sprintall, Z. Liu, W. Yu, A. Santoso, X.-H. Yan, and R. D. Susanto, "Previously unidenti-
225 fied Indonesian Throughflow pathways and freshening in the Indian Ocean during recent decades,"
226 *Scientific Reports*, vol. 9, no. 1, p. 7364, 2019.
- 227 [6] T. Nagai, T. Hibiya, and F. Syamsudin, "Direct estimates of turbulent mixing in the Indonesian
228 archipelago and its role in the transformation of the Indonesian throughflow waters," *Geophysical
229 Research Letters*, vol. 48, no. 6, p. e2020GL091731, 2021.

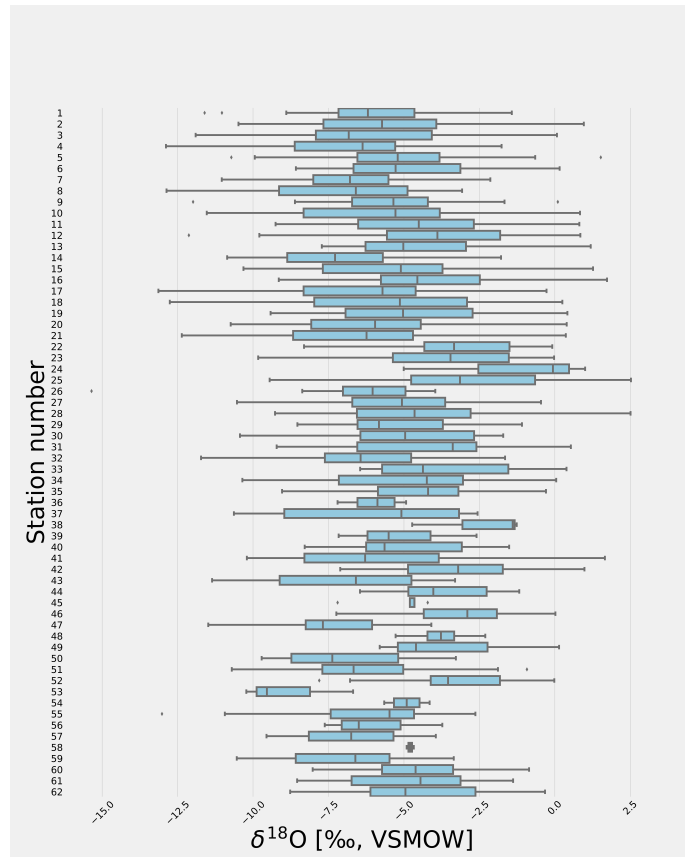
- 230 [7] A. Santoso, M. H. England, J. B. Kajtar, and W. Cai, "Indonesian Throughflow Variability and Linkage to
231 ENSO and IOD in an Ensemble of CMIP5 Models," *Journal of Climate*, vol. 35, no. 10, pp. 3161–3178,
232 2022.
- 233 [8] E. Aldrian and R. D. Susanto, "Identification of three dominant rainfall regions within Indonesia and
234 their relationship to sea surface temperature," *International Journal of Climatology*, vol. 23, no. 12,
235 pp. 1435–1452, 2003.
- 236 [9] C.-P. Chang, P. A. Harr, and H.-J. Chen, "Synoptic disturbances over the equatorial South China Sea and
237 western Maritime Continent during boreal winter," *Monthly Weather Review*, vol. 133, no. 3, pp. 489–
238 503, 2005.
- 239 [10] C.-P. Chang, Z. Wang, J. McBride, and C.-H. Liu, "Annual cycle of Southeast Asia—Maritime Continent
240 rainfall and the asymmetric monsoon transition," *Journal of Climate*, vol. 18, no. 2, pp. 287–301, 2005.
- 241 [11] S. C. Peatman, J. Schwendike, C. E. Birch, J. H. Marsham, A. J. Matthews, and G.-Y. Yang, "A local-to-
242 large scale view of Maritime Continent rainfall: Control by ENSO, MJO, and equatorial waves," *Journal*
243 *of Climate*, vol. 34, no. 22, pp. 8933–8953, 2021.
- 244 [12] J. Zhu, Z. Guan, and X. Wang, "Variations of Summertime SSTA Independent of ENSO in the Maritime
245 Continent and Their Possible Impacts on Rainfall in the Asian–Australian Monsoon Region," *Journal of*
246 *Climate*, vol. 35, no. 24, pp. 7949–7964, 2022.
- 247 [13] C. Chen, S. Sahany, A. F. Moise, X. R. Chua, M. E. Hassim, G. Lim, and V. Prasanna, "ENSO–Rainfall
248 Teleconnection over the Maritime Continent Enhances and Shifts Eastward under Warming," *Journal*
249 *of Climate*, vol. 36, no. 14, pp. 4635–4663, 2023.
- 250 [14] C. Gao and G. Li, "Asymmetric effect of enso on the maritime continent precipitation in decaying sum-
251 mers," *Climate Dynamics*, vol. 61, p. 2839–2852, 2023.
- 252 [15] J. Lu, T. Li, and X. Shen, "Precipitation diurnal cycle over the maritime continent modulated by ENSO,"
253 *Climate Dynamics*, vol. 61, p. 2547–2564, 2023.
- 254 [16] C. Hu, T. Lian, H.-N. Cheung, S. Qiao, Z. Li, K. Deng, S. Yang, and D. Chen, "Mixed diversity of shifting
255 IOD and El Niño dominates the location of Maritime Continent autumn drought," *National Science*
256 *Review*, vol. 7, no. 7, pp. 1150–1153, 2020.
- 257 [17] H.-M. Xiao, M.-H. Lo, and J.-Y. Yu, "The increased frequency of combined El Niño and positive IOD
258 events since 1965s and its impacts on maritime continent hydroclimates," *Scientific Reports*, vol. 12,
259 no. 1, p. 7532, 2022.
- 260 [18] M.-S. Ahn, D. Kim, Y.-G. Ham, and S. Park, "Role of Maritime Continent land convection on the mean
261 state and MJO propagation," *Journal of Climate*, vol. 33, no. 5, pp. 1659–1675, 2020.
- 262 [19] Y. Wei, Z. Pu, and C. Zhang, "Diurnal cycle of precipitation over the Maritime Continent under modula-
263 tion of MJO: Perspectives from cloud-permitting scale simulations," *Journal of Geophysical Research:*
264 *Atmospheres*, vol. 125, no. 13, p. e2020JD032529, 2020.
- 265 [20] H. Bai and C. Schumacher, "Topographic influences on diurnally driven MJO rainfall over the Maritime
266 Continent," *Journal of Geophysical Research: Atmospheres*, vol. 127, no. 6, p. e2021JD035905, 2022.
- 267 [21] S. Abhik, H. H. Hendon, and C. Zhang, "The Indo-Pacific Maritime Continent Barrier Effect on MJO
268 Prediction," *Journal of Climate*, vol. 36, no. 3, pp. 945–957, 2023.
- 269 [22] J. Hudson and E. Maloney, "The Role of Surface Fluxes in MJO Propagation through the Maritime
270 Continent," *Journal of Climate*, vol. 36, no. 6, pp. 1633–1652, 2023.
- 271 [23] M. D. Yamanaka, "Physical climatology of Indonesian maritime continent: An outline to comprehend
272 observational studies," *Atmospheric Research*, vol. 178, pp. 231–259, 2016.
- 273 [24] F. Tritschler, M. Binder, F. Händel, D. Burghardt, P. Dietrich, and R. Liedl, "Collected Rain Water as
274 Cost-Efficient Source for Aquifer Tracer Testing," *Groundwater*, vol. 58, no. 1, pp. 125–131, 2020.
- 275 [25] S. Valdivielso, E. Vázquez-Suñé, and E. Custodio, "Origin and variability of oxygen and hydrogen iso-
276 topic composition of precipitation in the Central Andes: A review," *Journal of Hydrology*, vol. 587,
277 p. 124899, 2020.

- 278 [26] S. He, D. Jackisch, D. Samanta, P. K. Y. Yi, G. Liu, X. Wang, and N. F. Goodkin, "Understanding tropical
279 convection through triple oxygen isotopes of precipitation from the maritime continent," *Journal of*
280 *Geophysical Research: Atmospheres*, vol. 126, no. 4, p. e2020JD033418, 2021.
- 281 [27] F. Malik, S. Butt, and N. Mujahid, "Variation in isotopic composition of precipitation with identification
282 of vapor source using deuterium excess as tool," *Journal of Radioanalytical and Nuclear Chemistry*,
283 pp. 1–8, 2022.
- 284 [28] J. Bershaw, "Controls on deuterium excess across Asia," *Geosciences*, vol. 8, no. 7, p. 257, 2018.
- 285 [29] J. Y. Liu, F. P. Zhang, Q. Feng, Y. F. Wei, L. H. Huang, Z. X. Li, S. Nie, and L. Li, "Stable isotopes character-
286 istics of precipitation over shaanxi-gansu-ningxia and its water vapor sources," *The Journal of Applied*
287 *Ecology*, vol. 30, no. 7, pp. 2191–2200, 2019.
- 288 [30] C. C. Routson, N. P. McKay, D. S. Kaufman, M. P. Erb, H. Goosse, B. N. Shuman, J. R. Rodysill, and T. Ault,
289 "Mid-latitude net precipitation decreased with Arctic warming during the Holocene," *Nature*, vol. 568,
290 no. 7750, pp. 83–87, 2019.
- 291 [31] C. C. Xia, K. Chen, J. Zhou, J. Mei, Y. P. Liu, and G. D. Liu, "Comparison of precipitation stable isotopes
292 during wet and dry seasons in a subtropical monsoon climate region of China," *Applied Ecology &*
293 *Environmental Research*, vol. 17, no. 5, 2019.
- 294 [32] C. Xia, G. Liu, K. Chen, Y. Hu, J. Zhou, Y. Liu, and J. Mei, "Stable isotope characteristics for precipitation
295 events and their responses to moisture and environmental changes during the summer monsoon
296 period in southwestern china.," *Polish Journal of Environmental Studies*, vol. 29, no. 3, 2020.
- 297 [33] N. Kurita, K. Ichiyanagi, J. Matsumoto, M. D. Yamanaka, and T. Ohata, "The relationship between the
298 isotopic content of precipitation and the precipitation amount in tropical regions," *Journal of Geo-*
299 *chemical Exploration*, vol. 102, no. 3, pp. 113–122, 2009.
- 300 [34] N. C. Munksgaard, N. Kurita, R. Sánchez-Murillo, N. Ahmed, L. Araguas, D. L. Balachew, M. I. Bird,
301 S. Chakraborty, N. K. Chinh, K. M. Cobb, *et al.*, "Data descriptor: Daily observations of stable isotope
302 ratios of rainfall in the tropics," *Scientific reports*, vol. 9, no. 1, p. 14419, 2019.
- 303 [35] C. Xia, G. Liu, J. Mei, Y. Meng, W. Liu, and Y. Hu, "Characteristics of hydrogen and oxygen stable isotopes
304 in precipitation and the environmental controls in tropical monsoon climatic zone," *International Jour-*
305 *nal of Hydrogen Energy*, vol. 44, no. 11, pp. 5417–5427, 2019.
- 306 [36] D. Jackisch, B. X. Yeo, A. D. Switzer, S. He, D. L. M. Cantarero, F. P. Siringan, and N. F. Goodkin, "Pre-
307 cipitation stable isotopic signatures of tropical cyclones in Metropolitan Manila, Philippines, show
308 significant negative isotopic excursions," *Natural Hazards and Earth System Sciences*, vol. 22, no. 1,
309 pp. 213–226, 2022.
- 310 [37] W. Dansgaard, "Stable isotopes in precipitation," *Tellus*, vol. 16, no. 4, pp. 436–468, 1964.
- 311 [38] R. Suwarman, K. Ichiyanagi, M. Tanoue, K. Yoshimura, S. Mori, M. D. Yamanaka, N. Kurita, and F. Syam-
312 sudin, "The variability of stable isotopes and water origin of precipitation over the Maritime Conti-
313 nent," *SOLA*, vol. 9, pp. 74–78, 2013.
- 314 [39] H. A. Belgaman, K. Ichiyanagi, M. Tanoue, R. Suwarman, K. Yoshimura, S. Mori, N. Kurita, M. D. Ya-
315 manaka, and F. Syamsudin, "Intraseasonal variability of $\delta^{18}\text{O}$ of precipitation over the Indonesian
316 maritime continent related to the Madden-Julian oscillation," *SOLA*, vol. 12, pp. 192–197, 2016.
- 317 [40] R. Suwarman, K. Ichiyanagi, M. Tanoue, K. Yoshimura, S. Mori, M. D. Yamanaka, F. Syamsudin, and
318 H. A. Belgaman, "El niño southern oscillation signature in atmospheric water isotopes over maritime
319 continent during wet season," *Journal of the Meteorological Society of Japan. Ser. II*, vol. 95, no. 1,
320 pp. 49–66, 2017.
- 321 [41] M. N. Evans, S. E. Tolwinski-Ward, D. M. Thompson, and K. J. Anchukaitis, "Applications of proxy system
322 modeling in high resolution paleoclimatology," *Quaternary Science Reviews*, vol. 76, pp. 16–28, 2013.
- 323 [42] P. Peng, X. J. Zhang, and J. Chen, "Bias correcting isotope-equipped GCMs outputs to build precipita-
324 tion oxygen isoscape for eastern China," *Journal of Hydrology*, vol. 589, p. 125153, 2020.
- 325 [43] Y. Nan, Z. He, F. Tian, Z. Wei, and L. Tian, "Can we use precipitation isotope outputs of isotopic general
326 circulation models to improve hydrological modeling in large mountainous catchments on the Tibetan
327 Plateau?," *Hydrology and Earth System Sciences*, vol. 25, no. 12, pp. 6151–6172, 2021.

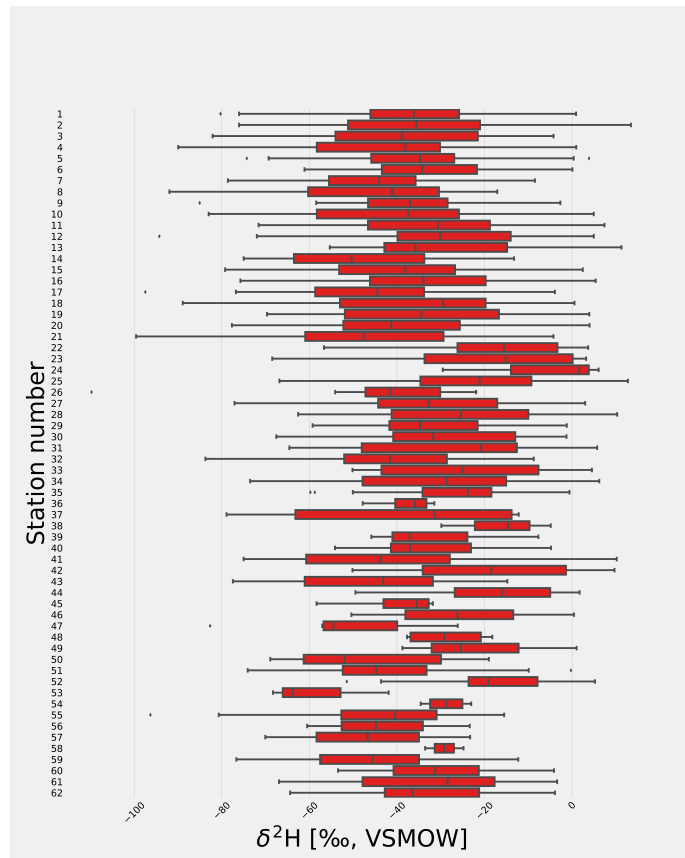
- 328 [44] J. Chen, J. Chen, X. J. Zhang, P. Peng, and C. Risi, "A 148-year precipitation oxygen isoscape for China
329 generated based on data fusion and bias correction of iGCMs simulations," *Earth System Science Data*
330 *Discussions*, pp. 1–27, 2022.
- 331 [45] J. Chen, J. Chen, X. J. Zhang, P. Peng, and C. Risi, "A century and a half precipitation oxygen isoscape
332 for China generated using data fusion and bias correction," *Scientific Data*, vol. 10, no. 1, p. 185, 2023.
- 333 [46] H. A. Belgaman, K. Ichiyanagi, M. Tanoue, and R. Suwarman, "Observational research on stable iso-
334 topes in precipitation over Indonesian maritime continent," *Nihon Suimon Kagaku Kaishi (Online)*,
335 vol. 46, no. 1, pp. 7–28, 2016.
- 336 [47] H. A. Belgaman, K. Ichiyanagi, R. Suwarman, M. Tanoue, E. Aldrian, A. I. D. Utami, and S. D. A. Kusuman-
337 ingyas, "Characteristics of seasonal precipitation isotope variability in Indonesia," *Hydrological Re-*
338 *search Letters*, vol. 11, no. 2, pp. 92–98, 2017.
- 339 [48] J. Perkel, "Democratic databases: science on GitHub," *Nature*, vol. 538, no. 7623, pp. 127–128, 2016.
- 340 [49] P. Wessel, J. F. Luis, L. Uieda, R. Scharroo, F. Wobbe, W. H. F. Smith, and D. Tian, "The Generic Mapping
341 Tools Version 6," *Geochemistry, Geophysics, Geosystems*, vol. 20, no. 11, pp. 5556–5564, 2019.
- 342 [50] L. Uieda, D. Tian, W. J. Leong, W. Schlitzer, M. Grund, M. Jones, Y. Fröhlich, L. Toney, J. Yao, Y. Magen,
343 J.-H. Tong, K. Materna, A. Belem, T. Newton, A. Anant, M. Ziebarth, J. Quinn, and P. Wessel, "PyGMT: A
344 Python interface for the Generic Mapping Tools," 2023. Software available from [https://doi.org/
345 10.5281/zenodo.7772533](https://doi.org/10.5281/zenodo.7772533).
- 346 [51] S. De Graaf, H. B. Vonhof, T. Weissbach, J. A. Wassenburg, E. J. Levy, T. Kluge, and G. H. Haug, "A
347 comparison of isotope ratio mass spectrometry and cavity ring-down spectroscopy techniques for
348 isotope analysis of fluid inclusion water," *Rapid Communications in Mass Spectrometry*, vol. 34, no. 16,
349 p. e8837, 2020.
- 350 [52] S. Maithani and M. Pradhan, "Cavity ring-down spectroscopy and its applications to environmental,
351 chemical and biomedical systems," *Journal of Chemical Sciences*, vol. 132, pp. 1–19, 2020.
- 352 [53] H. Sagayama, N. M. Racine, T. C. Shriver, and D. A. Schoeller, "Comparison of isotope ratio mass spec-
353 trometry and cavity ring-down spectroscopy procedures and precision of the doubly labeled water
354 method in different physiological specimens," *Rapid Communications in Mass Spectrometry*, vol. 35,
355 no. 21, p. e9188, 2021.
- 356 [54] J. A. Hutchings and B. L. Konecky, "Optimization of a Picarro L2140-i cavity ring-down spectrometer for
357 routine measurement of triple oxygen isotope ratios in meteoric waters," *Atmospheric Measurement*
358 *Techniques*, vol. 16, no. 6, pp. 1663–1682, 2023.
- 359 [55] J. Zhang and Z. Xu, "Vacuum extraction of high-salinity water for the determination of oxygen and hy-
360 drogen isotopic compositions using cavity ring-down spectroscopy," *Microchemical Journal*, vol. 190,
361 p. 108678, 2023.
- 362 [56] G. M. Hornberger, "New manuscript guidelines for the reporting of stable hydrogen, carbon, and oxy-
363 gen isotope ratio data," *Water Resources Research*, vol. 31, no. 12, pp. 2895–2895, 1995.
- 364 [57] T. B. Coplen, "Normalization of oxygen and hydrogen isotope data," *Chemical Geology: Isotope Geo-*
365 *science Section*, vol. 72, no. 4, pp. 293–297, 1988.
- 366 [58] D. Taylor, "Work the shell: analyzing comma-separated values (csv) files," *Linux Journal*, vol. 2015,
367 no. 260, p. 3, 2015.
- 368 [59] S. Mäs, D. Henzen, L. Bernard, M. Müller, S. Jirka, and I. Senner, "Generic schema descriptions for
369 comma-separated values files of environmental data," in *The 21th AGILE International Conference on*
370 *Geographic Information Science*, 2018.
- 371 [60] H. Craig, "Isotopic variations in meteoric waters," *Science*, vol. 133, no. 3465, pp. 1702–1703, 1961.
- 372 [61] L. Merlivat and J. Jouzel, "Global climatic interpretation of the deuterium-oxygen 18 relationship for
373 precipitation," *Journal of Geophysical Research: Oceans*, vol. 84, no. C8, pp. 5029–5033, 1979.
- 374 [62] S. Pfahl and H. Sodemann, "What controls deuterium excess in global precipitation?," *Climate of the*
375 *Past*, vol. 10, no. 2, pp. 771–781, 2014.

- 376 [63] R. Sánchez-Murillo, A. M. Durán-Quesada, C. Birkel, G. Esquivel-Hernández, and J. Boll, “Tropical pre-
377 cipitation anomalies and d-excess evolution during El Niño 2014-16,” *Hydrological Processes*, vol. 31,
378 no. 4, pp. 956–967, 2017.
- 379 [64] K. Yoshikawa, J. Úbeda, P. Masías, W. Pari, F. Apaza, P. Vasquez, B. Ccallata, R. Concha, G. Luna, J. Ipar-
380 raguirre, *et al.*, “Current thermal state of permafrost in the southern Peruvian Andes and potential
381 impact from El Niño–Southern Oscillation (ENSO),” *Permafrost and Periglacial Processes*, vol. 31, no. 4,
382 pp. 598–609, 2020.
- 383 [65] L. Shao, L. Tian, Z. Cai, C. Wang, and Y. Li, “Large-scale atmospheric circulation influences the ice core
384 d-excess record from the central Tibetan Plateau,” *Climate Dynamics*, vol. 57, no. 7-8, pp. 1805–1816,
385 2021.
- 386 [66] S. Van Der Walt, S. C. Colbert, and G. Varoquaux, “The NumPy array: a structure for efficient numerical
387 computation,” *Computing in science & engineering*, vol. 13, no. 2, pp. 22–30, 2011.
- 388 [67] W. McKinney *et al.*, “pandas: a foundational Python library for data analysis and statistics,” *Python for
389 high performance and scientific computing*, vol. 14, no. 9, pp. 1–9, 2011.
- 390 [68] K. Rozanski, L. Araguás-Araguás, and R. Gonfiantini, “Isotopic patterns in modern global precipitation,”
391 *Climate change in continental isotopic records*, vol. 78, pp. 1–36, 1993.
- 392 [69] A. L. Putman, R. P. Fiorella, G. J. Bowen, and Z. Cai, “A global perspective on local meteoric water lines:
393 Meta-analytic insight into fundamental controls and practical constraints,” *Water Resources Research*,
394 vol. 55, no. 8, pp. 6896–6910, 2019.
- 395 [70] L. N. Arellano, S. P. Good, R. Sánchez-Murillo, W. T. Jarvis, D. C. Noone, and C. E. Finkenbiner, “Bayesian
396 estimates of the mean recharge elevations of water sources in the Central America region using stable
397 water isotopes,” *Journal of Hydrology: Regional Studies*, vol. 32, p. 100739, 2020.
- 398 [71] J. A. Torres-Martínez, A. Mora, P. S. K. Knappett, N. Ornelas-Soto, and J. Mahlknecht, “Tracking nitrate
399 and sulfate sources in groundwater of an urbanized valley using a multi-tracer approach combined
400 with a bayesian isotope mixing model,” *Water Research*, vol. 182, p. 115962, 2020.
- 401 [72] Q. Zhang, H. Wang, and C. Lu, “Tracing sulfate origin and transformation in an area with multiple
402 sources of pollution in northern China by using environmental isotopes and Bayesian isotope mixing
403 model,” *Environmental Pollution*, vol. 265, p. 115105, 2020.
- 404 [73] X. Kang, Y. Niu, H. Yu, P. Gou, Q. Hou, X. Lu, and Y. Wu, “Effect of rainfall-runoff process on sources and
405 transformations of nitrate using a combined approach of dual isotopes, hydrochemical and Bayesian
406 model in the Dagang River basin,” *Science of the Total Environment*, vol. 837, p. 155674, 2022.
- 407 [74] A. Zaryab, H. R. Nassery, K. Knoeller, F. Alijani, and E. Minet, “Determining nitrate pollution sources in
408 the Kabul Plain aquifer (Afghanistan) using stable isotopes and Bayesian stable isotope mixing model,”
409 *Science of the Total Environment*, vol. 823, p. 153749, 2022.
- 410 [75] H. Mao, C. Wang, S. Qu, F. Liao, G. Wang, and Z. Shi, “Source and evolution of sulfate in the multi-
411 layer groundwater system in an abandoned mine—Insight from stable isotopes and Bayesian isotope
412 mixing model,” *Science of the Total Environment*, vol. 859, p. 160368, 2023.
- 413 [76] K. Klauenberg, G. Wübbeler, B. Mickan, P. Harris, and C. Elster, “A tutorial on Bayesian normal linear
414 regression,” *Metrologia*, vol. 52, no. 6, p. 878, 2015.
- 415 [77] M. West, “Outlier models and prior distributions in Bayesian linear regression,” *Journal of the Royal
416 Statistical Society Series B: Statistical Methodology*, vol. 46, no. 3, pp. 431–439, 1984.
- 417 [78] G. L. Jones and Q. Qin, “Markov chain Monte Carlo in practice,” *Annual Review of Statistics and Its
418 Application*, vol. 9, pp. 557–578, 2022.
- 419 [79] N. Metropolis, A. W. Rosenbluth, M. N. Rosenbluth, A. H. Teller, and E. Teller, “Equation of state cal-
420 culations by fast computing machines,” *The Journal of Chemical Physics*, vol. 21, no. 6, pp. 1087–1092,
421 1953.
- 422 [80] W. K. Hastings, “Monte Carlo sampling methods using Markov chains and their applications,”
423 *Biometrika*, vol. 57, no. 1, pp. 97–109, 1970.

- 424 [81] S. Chib and E. Greenberg, "Understanding the Metropolis-Hastings Algorithm," *The American Statistician*, vol. 49, no. 4, pp. 327–335, 1995.
425
- 426 [82] Y. Fan, X. Shi, Q. Duan, and L. Yu, "Towards reliable uncertainty quantification for hydrologic predic-
427 tions, Part I: Development of a particle copula Metropolis Hastings method," *Journal of Hydrology*,
428 vol. 612, p. 128163, 2022.
- 429 [83] S. Herho, F. Fajary, and D. Irawan, "On the Statistical Learning Analysis of Rain Gauge Data over the
430 Natuna Islands," *Indonesian Journal of Statistics and Its Applications*, vol. 6, no. 2, pp. 347–357, 2022.
- 431 [84] S. H. S. Herho, "A Univariate Extreme Value Analysis and Change Point Detection of Monthly Discharge
432 in Kali Kupang, Central Java, Indonesia," *JOIV: International Journal on Informatics Visualization*, vol. 6,
433 no. 4, pp. 862–868, 2022.
- 434 [85] S. Sharma and P. P. Mujumdar, "Modeling concurrent hydroclimatic extremes with parametric multi-
435 variate extreme value models," *Water Resources Research*, vol. 58, no. 2, p. e2021WR031519, 2022.
- 436 [86] R. Vinnarasi and C. T. Dhanya, "Time-varying Intensity-Duration-Frequency relationship through
437 climate-informed covariates," *Journal of Hydrology*, vol. 604, p. 127178, 2022.
- 438 [87] H. Xu, S. Song, T. Guo, and H. Wang, "Two-stage hybrid model for hydrological series prediction based
439 on a new method of partitioning datasets," *Journal of Hydrology*, vol. 612, p. 128122, 2022.
- 440 [88] B. Zolghadr-Asli, O. Bozorg-Haddad, M. Enayati, and H. A. Loáiciga, "Sensitivity of non-conditional
441 climatic variables to climate-change deep uncertainty using Markov Chain Monte Carlo simulation,"
442 *Scientific Reports*, vol. 12, no. 1, p. 1813, 2022.
- 443 [89] L. F. South, M. Riabiz, O. Teymur, and C. J. Oates, "Postprocessing of MCMC," *Annual Review of Statis-
444 tics and Its Application*, vol. 9, pp. 529–555, 2022.
- 445 [90] C. Karras, A. Karras, M. Avlonitis, and S. Sioutas, "An overview of mcmc methods: From theory to
446 applications," in *IFIP International Conference on Artificial Intelligence Applications and Innovations*,
447 pp. 319–332, Springer, 2022.
- 448 [91] S. Agrawal, D. Vats, K. Łatuszyński, and G. O. Roberts, "Optimal scaling of MCMC beyond Metropolis,"
449 *Advances in Applied Probability*, vol. 55, no. 2, pp. 492–509, 2023.
- 450 [92] J. Salvatier, T. V. Wiecki, and C. Fonnesbeck, "Probabilistic programming in Python using PyMC3," *PeerJ
451 Computer Science*, vol. 2, p. e55, 2016.
- 452 [93] Supari, F. Tangang, E. Salimun, E. Aldrian, A. Sopaheluwakan, and L. Juneng, "ENSO modulation of
453 seasonal rainfall and extremes in Indonesia," *Climate Dynamics*, vol. 51, pp. 2559–2580, 2018.
- 454 [94] T. Ferijal, O. Batelaan, and M. Shanafield, "Spatial and temporal variation in rainy season droughts in
455 the Indonesian Maritime Continent," *Journal of Hydrology*, vol. 603, p. 126999, 2021.
- 456 [95] S. He, N. F. Goodkin, D. Jackisch, M. R. Ong, and D. Samanta, "Continuous real-time analysis of the
457 isotopic composition of precipitation during tropical rain events: Insights into tropical convection,"
458 *Hydrological Processes*, vol. 32, no. 11, pp. 1531–1545, 2018.
- 459 [96] S. He, N. F. Goodkin, N. Kurita, X. Wang, and C. M. Rubin, "Stable isotopes of precipitation during
460 tropical Sumatra Squalls in Singapore," *Journal of Geophysical Research: Atmospheres*, vol. 123, no. 7,
461 pp. 3812–3829, 2018.
- 462 [97] C. Funk, P. Peterson, M. Landsfeld, D. Pedreros, J. Verdin, S. Shukla, G. Husak, J. Rowland, L. Harrison,
463 A. Hoell, *et al.*, "The climate hazards infrared precipitation with stations—a new environmental record
464 for monitoring extremes," *Scientific data*, vol. 2, no. 1, pp. 1–21, 2015.

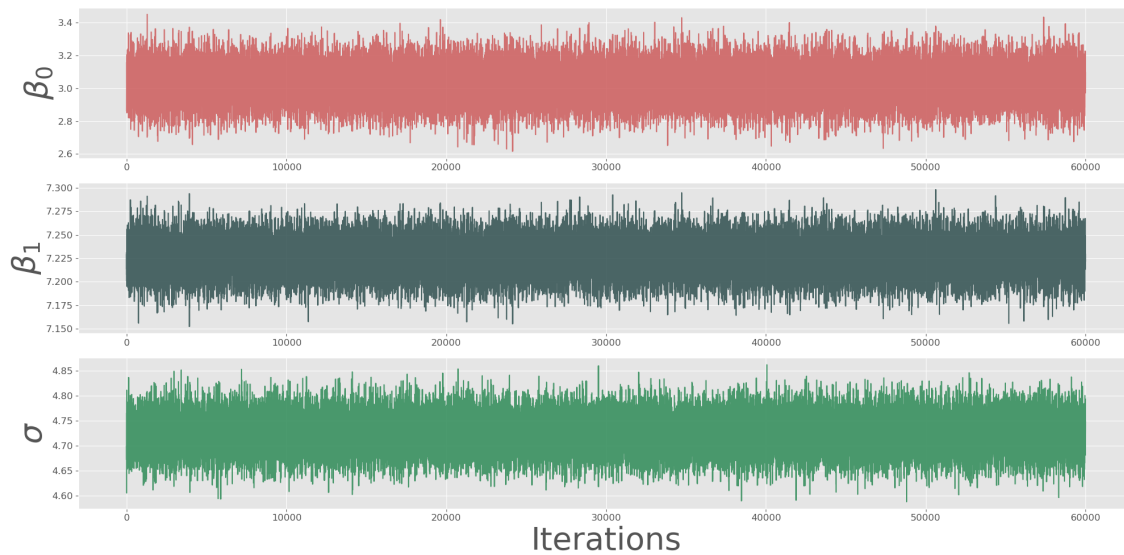


(a)

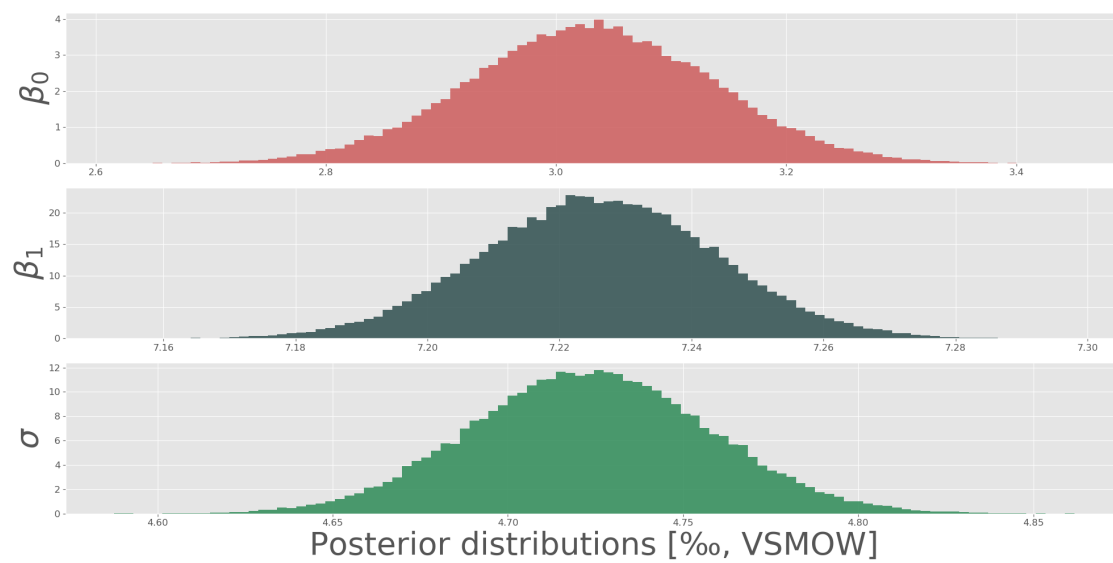


(b)

Figure 3: Box plots of the monthly (a) $\delta^{18}\text{O}$ and (b) $\delta^2\text{H}$ recorded by the 62 stations between September 2010 and September 2017.



(a)



(b)

Figure 4: (a) BLR posterior parameter trace plots for the intercept (upper panel), slope (middle panel), and standard deviation (lower panel). (b) Posterior distribution of the three linear regression parameters: intercept (upper panel), slope (middle panel), and standard deviation (lower panel).

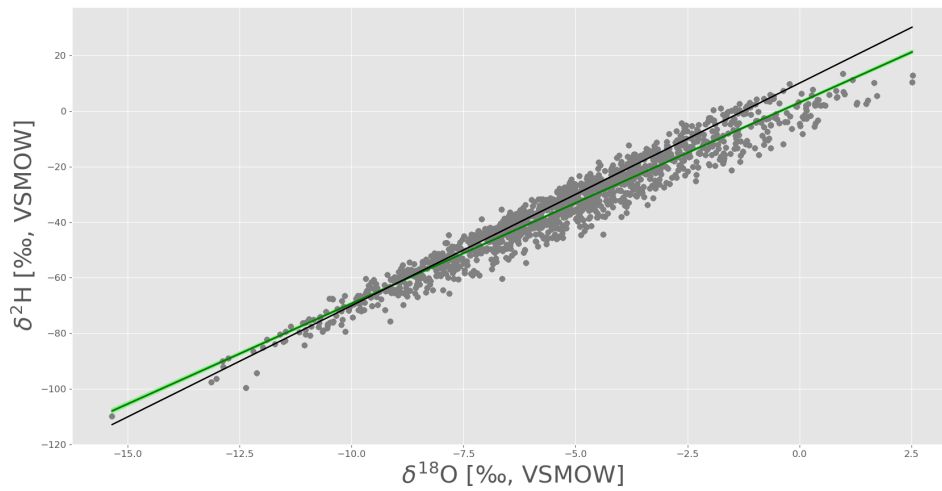


Figure 5: The GMWL (solid black line) compared to the LMWL (the posterior mean shown by a solid green line, light green area shows 95% credible interval obtained from the highest posterior density interval (HPDI)) of all stations over the IMC. Grey dots indicate individual data points.

imc-precip-iso: Open monthly stable isotope data of precipitation over the Indonesian Maritime Continent

R. Suwarman¹, S. H. S. Herho^{2,3,*}, H. A. Belgaman⁴, K. Ichiyanagi⁵, T. Uesugi⁵, D. E. Irawan⁶, I. M. Yosa¹, A. I. D. Utami⁷, S. Prayogo⁸, and E. Aldrian⁴

¹Atmospheric Science Research Group, Bandung Institute of Technology (ITB), Bandung, Indonesia

²Department of Earth and Planetary Sciences, University of California, Riverside, USA

³Department of Geology, University of Maryland, College Park, USA

⁴Research Center for Climate and Atmosphere (PRIMA), National Research and Innovation Agency (BRIN), Bandung, Indonesia

⁵Faculty of Advanced Science and Technology, Kumamoto University, Kumamoto, Japan

⁶Applied Geology Research Group, Bandung Institute of Technology (ITB), Bandung, Indonesia

⁷Indonesian Meteorology, Climatology, and Geophysical Agency (BMKG), Jakarta, Indonesia

⁸Software Engineering Division, Manvis Teknologi Enjinereng, Bandung, Indonesia

*Corresponding author: sandy.herho@email.ucr.edu

Abstract

Stable isotopes, $\delta^2\text{H}$, $\delta^{18}\text{O}$, and d-excess, are valuable tools as natural tracers of diffusion processes and phase changes in the global hydroclimatological cycle. The Indonesian Maritime Continent (IMC) is an archipelago area surrounded by very warm waters which induce convective activities as the primary heat source driving global atmospheric circulation. Given the central role of IMC in this hydroclimatological cycle, comprehensive study and data collection on the stable isotopes of precipitation in this region is crucial.

In this study, we collected monthly stable isotope data from 62 stations spread throughout the Indonesian archipelago from September 2010 to September 2017. We cleaned the data and conducted quality control activities by comparing the Local Meteoric Water Line (LMWL) to previous studies in a similar climatic region. We shared these data openly on our GitHub repository, making them easier to update and interact with users in the future.

1 INTRODUCTION

Indonesian Maritime Continent (IMC) comprises a group of islands surrounded by the Indian and Pacific Oceans. The region's climate is influenced by its insular geography and its position near the Equator. Located in the western part of the Indo-Pacific warm pool (IPWP), IMC is a source of latent heat release and deep convection which drives the Hadley and Walker cells, thus playing an essential role in the earth's hydrological cycle (Yang et al., 2019; Xue et al., 2020). IMC is also the only link for warmed surface waters from the Pacific Ocean to the Indian Ocean through the Indonesian Throughflow (ITF), a surface flow component of the global ocean conveyor belt (e. g. Godfrey, 1996; Li et al., 2020; Makarim et al., 2019; Nagai et al., 2021; Santoso et al., 2022).

In general, IMC experiences two seasons, namely the wet and dry seasons, each in boreal winter - spring (November-March/NDJFM) and boreal summer - fall (May - September/MJJAS) (Aldrian and Susanto, 2003; Yang et al., 2019). During the wet season, there is warm sea surface temperature (SST) and heavy precipitation over the IMC, which is brought by the Asian winter monsoon, which is northeasterly to the north of the equator and northwesterly to the south of the equator, the opposite also happens in the dry season (Chang et al., 2005a,b; Yang et al., 2019). Besides the annual cycle, IMC precipitation is influenced by internal global atmosphere-ocean interactions, such as the El Niño Southern Oscillation (ENSO) (e. g.

Peatman et al., 2021; Zhu et al., 2022; Chen et al., 2023a; Gao and Li, 2023; Lu et al., 2023) and the Indian Ocean Dipole mode (IOD) (e. g. Yang et al., 2019; Hu et al., 2020; Peatman et al., 2021; Xiao et al., 2022). On an intra-annual scale, precipitation over the IMC is also influenced by the Madden-Julian Oscillation (MJO), which propagates from the Indian Ocean to the Pacific Ocean via IMC (e. g. Ahn et al., 2020; Wei et al., 2020; Peatman et al., 2021; Bai and Schumacher, 2022; Abhik et al., 2023; Hudson and Maloney, 2023).

Given the importance of IMC in understanding the earth's hydroclimatological phenomena (Yamanaka, 2016), investigation of precipitation characteristics is inevitable. One of the characteristics of precipitation that is important to investigate is the traditional water-stable isotopes of precipitation ($\delta^{18}\text{O}$ and $\delta^2\text{H}$) which are considered one of the natural tracers of hydrological cycles as a consequence of equilibrium and kinetic processes during phase transitions and diffusive processes (Tritschler et al., 2020; Valdivielso et al., 2020; He et al., 2021; Malik et al., 2022). In general, oxygen-18 ($\delta^{18}\text{O}$) and deuterium ($\delta^2\text{H}$) at mid- and high-latitudes are correlated with temperature (e. g. Bershaw, 2018; Liu et al., 2019; Routson et al., 2019; Xia et al., 2019b, 2020). However, in tropical regions such as the IMC, these two isotopic compositions show a negative correlation (e.g. Kurita et al., 2009; Munksgaard et al., 2019; Xia et al., 2019a; Jackisch et al., 2022) due to a rainout process known as the amount effect (Dansgaard, 1964). $\delta^{18}\text{O}$ can also be used as a signature of the water vapour transport process during ENSO and MJO over the IMC (Suwarman et al., 2013; Belgaman et al., 2016b; Suwarman et al., 2017). Observations of $\delta^{18}\text{O}$ and $\delta^2\text{H}$ in the tropics are also crucial to confirm the sensitivity of proxy precipitation observations in paleoclimatology using proxy system modelling (PSM), which requires modern precipitation isotope data in the region (Evans et al., 2013). Modern precipitation isotope observations are also needed to correct calculations performed by isotope-enabled General Circulation Models (iGCMs) (e. g. Peng et al., 2020; Nan et al., 2021; Chen et al., 2022, 2023b).

Until recently, there is not much open and publicly accessible data on traditional precipitation isotope over the IMC. There are four isotope stations operated by the International Atomic Energy Agency (IAEA) within the framework of the Global Network of Isotopes in Precipitation (GNIP) program. However, these stations stopped operating in 2003 and only cover the Java region, except for the Jayapura station in Papua (Belgaman et al., 2016a). In addition, there were isotope observations conducted by the Institute of Observational Research for Global Change (IORGC)/Japan Agency for Marine-Earth Science and Technology (JAMSTEC) conducted at six stations across IMC between 2001 and 2007 (Kurita et al., 2009; Belgaman et al., 2016a).

In this study, we conducted monthly $\delta^{18}\text{O}$ and $\delta^2\text{H}$ sampling at 62 observation stations along the IMC from September 2010 to September 2017. Part of these data (30 stations) have been used in a study by Belgaman et al. (2017) but has yet to be opened to the public. We opened the $\delta^{18}\text{O}$ and $\delta^2\text{H}$ measurements to the public on our GitHub repository to support democratizing knowledge based on open-source code and reproducible datasets (Perkel, 2016).

2 DATA ACQUISITION

We conducted field sampling from 62 meteorological and climatological stations owned by the Indonesian Meteorology, Climatology, and Geophysical Agency (BMKG) throughout the IMC area (Figure 1). To find out the details of station numbering and their location, see the table on the following URL: https://github.com/sandyherho/imc-precip-iso/blob/main/output_data/sta_list.csv. We collected these precipitation samples manually using buckets and then put them into 6 mL glass vials with screw caps. To prevent secondary evaporation after storage, we discarded samples with a volume of less than 5 mL. We collected these monthly precipitation samples from September 2010 to September 2017.

We measured $\delta^{18}\text{O}$ and $\delta^2\text{H}$ using the Picarro[®] L2120-i instrument using the cavity ring-down spectroscopy technique, which has proven practical and accurate in measuring water isotopes (e. g. De Graaf et al., 2020; Maithani and Pradhan, 2020; Sagayama et al., 2021; Hutchings and Konecky, 2023; Zhang and Xu, 2023). We measured the ratio of the abundance of the heavy to light isotopes (R), in the context of this study, $^2\text{H}/^1\text{H}$ and $^{18}\text{O}/^{16}\text{O}$, from samples by comparing them to the international standard, namely the Vienna Standard Mean Ocean Water (VSMOW) (Hornberger, 1995) so that δ values were obtained in units per mil (‰) using the following equation:

$$\delta = \left(\frac{R_{\text{sample}}}{R_{\text{standard}}} - 1 \right) \times 10^3 \quad (1)$$

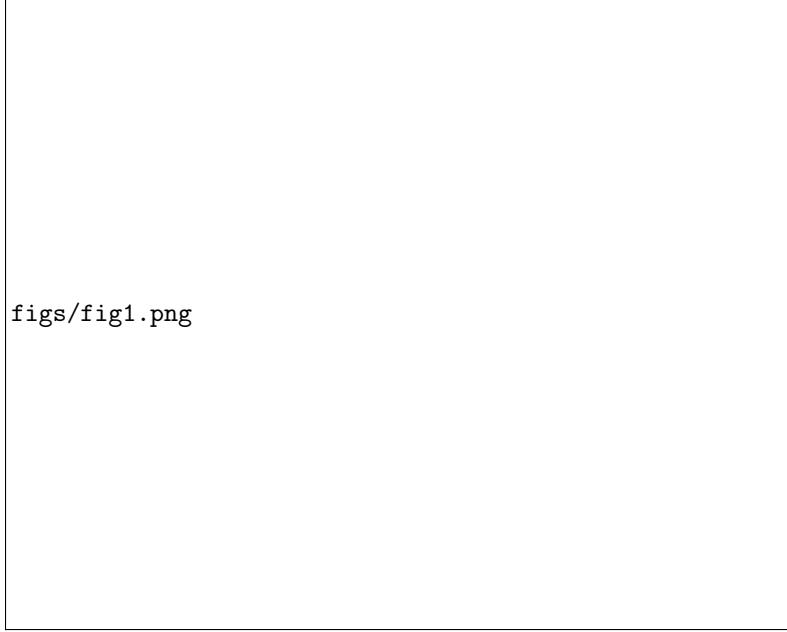


Figure 1: Location of the stations at which monthly samples of precipitation were collected for isotope measurements over the IMC (rendered using **PyGMT** (Wessel et al., 2019; Uieda et al., 2023)).

Due to the limited supply of international standards (is), we calibrated the samples (x) using three working standards (ws), Aqua Standard[®], SLW2 and ICE2, which had been calibrated against VSMOW. This calculation process is formulated through the following equation (Coplen, 1988):

$$\delta_{x-is} = \delta_{x-ws} + \delta_{ws-is} + (\delta_{x-ws} \times \delta_{ws-is}) \times 10^{-3} \quad (2)$$

Long-term standard errors (1σ) for these $\delta^{18}\text{O}$ and $\delta^2\text{H}$ measurements are $\pm 0.2\text{‰}$ and $\pm 1.0\text{‰}$, respectively.

Microsoft[®] Excel files extracted from the isotope measurement instrument were then converted into a text-formatted files, i. e. comma-separated values (CSV) format to make them easier to read by various kinds of software without being limited by a paid license (Taylor, 2015; Mäs et al., 2018). These data were then splitted into time series for each station and the entire IMC. In addition, we also calculated d-excess (d), which is defined as the deviation from $\delta^2\text{H}$ to $\delta^{18}\text{O}$ according to the definition of the Global Meteoric Water Line (GMWL) (Craig, 1961), which can be written as follows:

$$d = \delta^2\text{H} - 8\delta^{18}\text{O} \quad (3)$$

Calculation of this d-excess is necessary, given its correlation with the oceanic source of precipitation (Merliwat and Jouzel, 1979; Bershaw, 2018). Globally, this d-excess is a dependent variable of the relative humidity of the sea surface (Pfahl and Sodemann, 2014). Using d-excess, we can find the moisture flux anomaly during extreme events, such as ENSO influences in precipitation (e. g. Sánchez-Murillo et al., 2017; Yoshikawa et al., 2020; Shao et al., 2021). We did the entire data wrangling process using **NumPy** (Van Der Walt et al., 2011) and **pandas** (McKinney et al., 2011) libraries in the Python computing environment.

3 METHOD

We performed Local Meteoric Water Line (LMWL) calculations as part of our quality control efforts. It has been known since a study conducted by Craig (1961) that there is a linear relationship between $\delta^2\text{H}$ to $\delta^{18}\text{O}$ globally, which can be formulated as follows:

$$\delta^2\text{H} = 8\delta^{18}\text{O} + 10 \quad (4)$$

However, local slope variations and intercepts were only discovered after collecting IAEA/GNIP observations through the study of Rozanski et al. (1993), better known as LMWL. In this study, it is emphasized

that the relationship between the two isotopes is still linear. Variations in the slope may store information about the local seasonal climatology (Putman et al., 2019).

We used Bayesian Linear Regression (BLR) to determine the relationship between $\delta^2\text{H}$ and $\delta^{18}\text{O}$ over the IMC. BLR allows better handling of uncertainty in models. This method recognizes that we need perfect information about model parameters or data variability. We can represent this uncertainty using a probability distribution on the parameters in the Bayesian approach. This approach helps generate more realistic and credible parameter estimates and confidence intervals. The BLR approach allows us to incorporate any prior knowledge about the model parameters. This is useful when we need more data or want to use existing domain knowledge. In this study, we determined the priors for slopes and intercepts from the global data compilation for humid tropical regions (Köppen class A) that was done by Putman et al. (2019). Apart from single-point estimates (as in "frequentist" linear regression), the BLR gives a full posterior distribution of model parameters after looking at the data. This provides richer information about the parameter uncertainties and allows for more robust modelling of the $\delta^2\text{H}$ - $\delta^{18}\text{O}$ covariance. Because of these advantages, the Bayesian approaches have recently been popular for solving water isotope problems (e. g. Putman et al., 2019; Arellano et al., 2020; Torres-Martínez et al., 2020; Zhang et al., 2020; Kang et al., 2022; Zaryab et al., 2022; Mao et al., 2023). The full benefits of using BLR can be found in Klauenberg et al. (2015).

The simple linear regression model that we used to explain the statistical relationship between $\delta^2\text{H}$ and $\delta^{18}\text{O}$ is illustrated in the following equation:

$$\delta^2\text{H}_i = \beta_0 + \beta_1\delta^{18}\text{O}_i + \varepsilon_i \quad (5)$$

, where $\delta^2\text{H}_i$ and $\delta^{18}\text{O}_i$ are the observed deuterium and oxygen-18 isotope values for the i -th data point, respectively. β_0 and β_1 are the unknown regression coefficients (intercept and slope) to be estimated. ε_i is the random error term, assumed to be normally distributed, with mean zero and constant variance σ^2 .

BLR estimation started by specifying the prior distributions for the unknown parameters: β_0 , β_1 , and σ^2 . In this study, we assumed normal prior for intercept and slope, and uniform prior for variance (West, 1984):

$$\begin{cases} \beta_0 \sim \mathcal{N}(m_0, s_0^2) \\ \beta_1 \sim \mathcal{N}(m_1, s_1^2) \\ \sigma^2 \sim U(a, b) \end{cases} \quad (6)$$

Parameters m_0 , m_1 , s_0 , s_1 , a , and b were determined from the global observation database for the humid tropical regions (Köppen class A) (Putman et al., 2019).

Assuming errors ε_i are normally distributed, the likelihood function can be written in the following form:

$$p(\delta^2\text{H}_i | \beta_0, \beta_1, \delta^{18}\text{O}_i, \sigma^2) = \frac{1}{\sqrt{2\pi\sigma^2}} \exp\left(-\frac{(\delta^2\text{H}_i - \beta_0 - \beta_1\delta^{18}\text{O}_i)^2}{2\sigma^2}\right) \quad (7)$$

The joint posterior distribution of the BLR parameters given the observed isotope data ($\delta^2\text{H}_i, \delta^{18}\text{O}_i$) is:

$$p(\beta_0, \beta_1, \sigma^2 | \text{data}) \propto p(\text{data} | \beta_0, \beta_1, \sigma^2) \times p(\beta_0) \times p(\beta_1) \times p(\sigma^2) \quad (8)$$

, where $p(\text{data} | \beta_0, \beta_1, \sigma^2)$ is the likelihood and $p(\beta_0)$, $p(\beta_1)$, and $p(\sigma^2)$ are the priors.

We used a simple algorithm from the Markov chain Monte Carlo (MCMC) methods (Jones and Qin, 2022), the Metropolis-Hastings (MH) algorithm (Metropolis et al., 1953; Hastings, 1970), to estimate the posterior distribution. This algorithm can approximate the posterior distribution without the need to compute the normalization constant (Chib and Greenberg, 1995). MH algorithm has also proven reliable enough to be used in hydroclimatological problems (e. g. Putman et al., 2019; Fan et al., 2022; Herho, 2022; Sharma and Mujumdar, 2022; Vinnarasi and Dhanya, 2022; Xu et al., 2022; Zolghadr-Asli et al., 2022). MH algorithm can be summarized into several steps as follows:

1. Initialize the parameters $\beta_0^{(0)}$, $\beta_1^{(0)}$, and $\sigma_0^{2(0)}$ to some initial values.

2. For iteration $t = 1$ to T , where T is the number of iterations (in this study, we used 10,000 steps with the tuning of 2,000 steps which are the "burn in" iterations used to accelerate convergence (Jones and Qin, 2022; South et al., 2022)):

- (a) Calculate the acceptance ratio α :

$$\alpha = \frac{p(\text{data}|\beta_0, \beta_1, \sigma^{2*}) \times p(\beta_0) \times p(\beta_1) \times p(\sigma^{2*})}{p(\text{data}|\beta_0^{(t-1)}, \beta_1^{(t-1)}, \sigma^{2(t-1)}) \times p(\beta_0^{(t-1)}) \times p(\beta_1^{(t-1)}) \times p(\sigma^{2(t-1)})} \quad (9)$$

- (b) Generate a uniform random number u from $[0, 1]$.

- (c) If $u < \alpha$, accept the proposed parameters: $\beta_0^{(t)} = \beta_0, \beta_1^{(t)} = \beta_1, \sigma^{2(t)} = \sigma^{2*}$. Otherwise, keep the previous parameters: $\beta_0^{(t)} = \beta_0^{(t-1)}, \beta_1^{(t)} = \beta_1^{(t-1)}, \sigma^{2(t)} = \sigma^{2(t-1)}$.

3. After T iterations, we have samples from the posterior distribution. We use these samples to estimate the posterior mean, credible intervals, and other properties of the parameters.

This study uses a symmetrical Gaussian proposal distribution to simplify computing the acceptance ratio (Jones and Qin, 2022; Karras et al., 2022; South et al., 2022; Agrawal et al., 2023). We implemented the entire BLR process using the PyMC3 library within the Python computing environment (Salvatier et al., 2016).

4 RESULTS and DISCUSSION

The number of data points at each isotope observation station can be seen in Figure 2. The three stations with the most data collection were the Kemayoran Air Pollution Post in Jakarta (#1), with a total of 47 data points, followed by Deli Serdang in North Sumatra (#5) with a total of 46 data points, and in third place is the Bengkulu station (#11) which is located on the southwest coast of Sumatra with a total of 43 observations of data points. The stations with the fewest number of observations include Tambang (#57), located in Riau, and Ranomeeto (#58) in Southeast Sulawesi, each with two data points. Stations with the second-fewest number of observations include El Tari (#24) and Kupang in East Nusa Tenggara (#38), Mlati (#49) in Sleman, Yogyakarta, Malikusaleh (#53) in North Aceh, Koba (#56) in Bangka Belitung, each of which recorded only three data points. The stations with the third-fewest number of observations are Tarempa (#36) in the Riau Archipelago, West Seram (#48) in Maluku, and Sorong (#54) in Southwest Papua, each of which only has four data points. All stations' average and median data points were 21.968 and 22, respectively. These are very small because only about a quarter of the 85 months of observation period had successfully extracted $\delta^2\text{H}$ and $\delta^{18}\text{O}$ values.

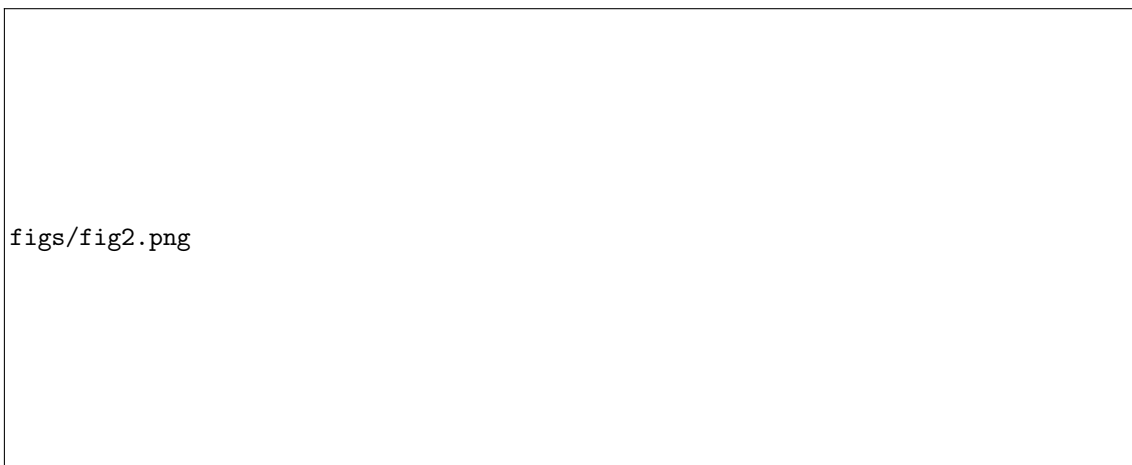


Figure 2: Availability of data points at each isotope station over the IMC collected in this study.

Weaknesses in data collection are also found in the need for more coverage of areas outside parts of Sumatra and Java due to limited access to transportation for sending samples. This must be underlined because most of the isotope measurements we produced in this study are concentrated in a region with monsoonal

rainfall classifications (Aldrian and Susanto, 2003; Supari et al., 2018; Ferijal et al., 2021). In contrast, anti-monsoonal and semi-annual regions are underrepresented. This is also evident in the less distribution of $\delta^2\text{H}$ and $\delta^{18}\text{O}$ values at stations in these two regions, as shown in the boxplots in Figure 3.

By combining $\delta^2\text{H}$ and $\delta^{18}\text{O}$ from all stations, we performed BLR inference, where the results of trace plots and the posterior distribution of the linear regression parameters can be seen in Figure 4. There is a convergence of all linear regression parameters, which can be visually seen in the trace plots (Figure 4a). The posterior distribution of the LMWL parameters that have been calculated using the MH algorithm is shown in Figure 4b. The mean and standard deviation of the posterior intercept are 3.506 ‰ and 1.732 ‰, respectively. Meanwhile, the mean and standard deviation of the posterior slope are 7.298 ‰ and 0.267 ‰, respectively. Then, for a 2σ credible interval, we can write the LMWL equation as follows:

$$\delta^2\text{H} = 7.298(\pm 0.534)\delta^{18}\text{O} + 3.506(\pm 3.464) \quad (10)$$

The two regression coefficients in Equation 10 are shallower when compared to GMWL. This indicates the occurrence of a sub-cloud evaporation process which indicates the occurrence of re-evaporation from rainwater after falling under the clouds through a tropical convective processes. Visually this can be seen by shifting the LMWL regression line clockwise when compared to the GMWL (Figure 5). Similar things were also found in previous studies over the Maritime Continent (He et al., 2018a,b, 2021).

5 CONCLUDING REMARKS

Based on water isotope observations from 62 stations that we collected from September 2010 to September 2017, we managed to build monthly $\delta^2\text{H}$, $\delta^{18}\text{O}$, and d-excess datasets per station and for all IMC, which are shared openly, accessible, and easily updated on the GitHub repository. We have also performed quality control on these data by calculating the LMWL using BLR, which is under the range of slopes and intercepts in previous studies conducted in areas with similar climate types (e. g. He et al., 2018a,b; Putman et al., 2019; He et al., 2021). The open data we shared are by far the most complete data over the IMC for stable isotopes of precipitation.

There are limitations to this study. One of them is that we should have checked the amount effect. This is due to the limitation of station precipitation data, which contains many empty data. In the future, a combination of station data and other high-resolution data sources is needed, such as the Climate Hazards Group InfraRed Precipitation with Station data (CHIRPS) (Funk et al., 2015), which can be used to calculate the amount effect. In addition, this monthly water isotope observation activities over the IMC were stopped in September 2017. This activity should be continued, given the central position of the IMC in the Earth's climate system, which is currently undergoing significant changes as a consequence of the unprecedented increase in anthropogenic radiative forcing. The study of water isotopes in precipitation over the IMC can undoubtedly deepen our understanding of anthropogenic and natural attributions in the hydrologic cycle in the tropics.

FUNDING

This study was supported by ITB Research, Community Service and Innovation Program (PPMI-ITB 2022) and Japan Society for the Promotion of Science (JSPS) KAKENHI (#24510256 and #16H05619).

DATA AVAILABILITY STATEMENT

All relevant code and data are available from this GitHub repository: <https://github.com/sandyherho/imc-precip-iso>.

CONFLICT OF INTEREST

The authors declare there is no conflict.

References

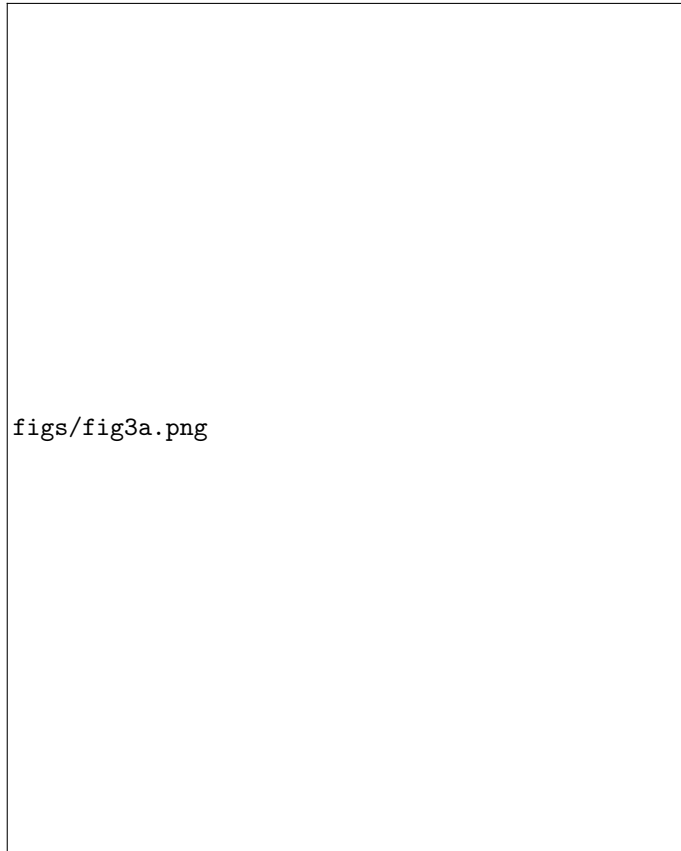
- Abhik, S., Hendon, H. H., and Zhang, C. (2023). The Indo-Pacific Maritime Continent Barrier Effect on MJO Prediction. *Journal of Climate*, 36(3):945–957.
- Agrawal, S., Vats, D., Łatuszyński, K., and Roberts, G. O. (2023). Optimal scaling of MCMC beyond Metropolis. *Advances in Applied Probability*, 55(2):492–509.
- Ahn, M.-S., Kim, D., Ham, Y.-G., and Park, S. (2020). Role of Maritime Continent land convection on the mean state and MJO propagation. *Journal of Climate*, 33(5):1659–1675.
- Aldrian, E. and Susanto, R. D. (2003). Identification of three dominant rainfall regions within Indonesia and their relationship to sea surface temperature. *International Journal of Climatology*, 23(12):1435–1452.
- Arellano, L. N., Good, S. P., Sánchez-Murillo, R., Jarvis, W. T., Noone, D. C., and Finkenbiner, C. E. (2020). Bayesian estimates of the mean recharge elevations of water sources in the Central America region using stable water isotopes. *Journal of Hydrology: Regional Studies*, 32:100739.
- Bai, H. and Schumacher, C. (2022). Topographic influences on diurnally driven MJO rainfall over the Maritime Continent. *Journal of Geophysical Research: Atmospheres*, 127(6):e2021JD035905.
- Belgaman, H. A., Ichianagi, K., Suwarman, R., Tanoue, M., Aldrian, E., Utami, A. I. D., and Kusumaningtyas, S. D. A. (2017). Characteristics of seasonal precipitation isotope variability in Indonesia. *Hydrological Research Letters*, 11(2):92–98.
- Belgaman, H. A., Ichianagi, K., Tanoue, M., and Suwarman, R. (2016a). Observational research on stable isotopes in precipitation over Indonesian maritime continent. *Nihon Suimon Kagaku Kaishi (Online)*, 46(1):7–28.
- Belgaman, H. A., Ichianagi, K., Tanoue, M., Suwarman, R., Yoshimura, K., Mori, S., Kurita, N., Yamanaka, M. D., and Syamsudin, F. (2016b). Intraseasonal variability of $\delta^{18}\text{O}$ of precipitation over the Indonesian maritime continent related to the Madden-Julian oscillation. *SOLA*, 12:192–197.
- Bershaw, J. (2018). Controls on deuterium excess across Asia. *Geosciences*, 8(7):257.
- Chang, C.-P., Harr, P. A., and Chen, H.-J. (2005a). Synoptic disturbances over the equatorial South China Sea and western Maritime Continent during boreal winter. *Monthly Weather Review*, 133(3):489–503.
- Chang, C.-P., Wang, Z., McBride, J., and Liu, C.-H. (2005b). Annual cycle of Southeast Asia—Maritime Continent rainfall and the asymmetric monsoon transition. *Journal of Climate*, 18(2):287–301.
- Chen, C., Sahany, S., Moise, A. F., Chua, X. R., Hassim, M. E., Lim, G., and Prasanna, V. (2023a). ENSO–Rainfall Teleconnection over the Maritime Continent Enhances and Shifts Eastward under Warming. *Journal of Climate*, 36(14):4635–4663.
- Chen, J., Chen, J., Zhang, X. J., Peng, P., and Risi, C. (2022). A 148-year precipitation oxygen isoscape for China generated based on data fusion and bias correction of iGCMs simulations. *Earth System Science Data Discussions*, pages 1–27.
- Chen, J., Chen, J., Zhang, X. J., Peng, P., and Risi, C. (2023b). A century and a half precipitation oxygen isoscape for China generated using data fusion and bias correction. *Scientific Data*, 10(1):185.
- Chib, S. and Greenberg, E. (1995). Understanding the Metropolis-Hastings Algorithm. *The American statistician*, 49(4):327–335.
- Coplen, T. B. (1988). Normalization of oxygen and hydrogen isotope data. *Chemical Geology: Isotope Geoscience Section*, 72(4):293–297.
- Craig, H. (1961). Isotopic variations in meteoric waters. *Science*, 133(3465):1702–1703.
- Dansgaard, W. (1964). Stable isotopes in precipitation. *Tellus*, 16(4):436–468.
- De Graaf, S., Vonhof, H. B., Weissbach, T., Wassenburg, J. A., Levy, E. J., Kluge, T., and Haug, G. H. (2020). A comparison of isotope ratio mass spectrometry and cavity ring-down spectroscopy techniques for isotope analysis of fluid inclusion water. *Rapid Communications in Mass Spectrometry*, 34(16):e8837.
- Evans, M. N., Tolwinski-Ward, S. E., Thompson, D. M., and Anchukaitis, K. J. (2013). Applications of proxy system modeling in high resolution paleoclimatology. *Quaternary Science Reviews*, 76:16–28.

- Fan, Y., Shi, X., Duan, Q., and Yu, L. (2022). Towards reliable uncertainty quantification for hydrologic predictions, Part I: Development of a particle copula Metropolis Hastings method. *Journal of Hydrology*, 612:128163.
- Ferijal, T., Batelaan, O., and Shanafield, M. (2021). Spatial and temporal variation in rainy season droughts in the Indonesian Maritime Continent. *Journal of Hydrology*, 603:126999.
- Funk, C., Peterson, P., Landsfeld, M., Pedreros, D., Verdin, J., Shukla, S., Husak, G., Rowland, J., Harrison, L., Hoell, A., et al. (2015). The climate hazards infrared precipitation with stations—a new environmental record for monitoring extremes. *Scientific data*, 2(1):1–21.
- Gao, C. and Li, G. (2023). Asymmetric effect of enso on the maritime continent precipitation in decaying summers. *Climate Dynamics*, 61:2839–2852.
- Godfrey, J. S. (1996). The effect of the Indonesian throughflow on ocean circulation and heat exchange with the atmosphere: A review. *Journal of Geophysical Research: Oceans*, 101(C5):12217–12237.
- Hastings, W. K. (1970). Monte Carlo sampling methods using Markov chains and their applications. *Biometrika*, 57(1):97–109.
- He, S., Goodkin, N. F., Jackisch, D., Ong, M. R., and Samanta, D. (2018a). Continuous real-time analysis of the isotopic composition of precipitation during tropical rain events: Insights into tropical convection. *Hydrological Processes*, 32(11):1531–1545.
- He, S., Goodkin, N. F., Kurita, N., Wang, X., and Rubin, C. M. (2018b). Stable isotopes of precipitation during tropical Sumatra Squalls in Singapore. *Journal of Geophysical Research: Atmospheres*, 123(7):3812–3829.
- He, S., Jackisch, D., Samanta, D., Yi, P. K. Y., Liu, G., Wang, X., and Goodkin, N. F. (2021). Understanding tropical convection through triple oxygen isotopes of precipitation from the maritime continent. *Journal of Geophysical Research: Atmospheres*, 126(4):e2020JD033418.
- Herho, S. H. S. (2022). A Univariate Extreme Value Analysis and Change Point Detection of Monthly Discharge in Kali Kupang, Central Java, Indonesia. *JOIV: International Journal on Informatics Visualization*, 6(4):862–868.
- Hornberger, G. M. (1995). New manuscript guidelines for the reporting of stable hydrogen, carbon, and oxygen isotope ratio data. *Water Resources Research*, 31(12):2895–2895.
- Hu, C., Lian, T., Cheung, H.-N., Qiao, S., Li, Z., Deng, K., Yang, S., and Chen, D. (2020). Mixed diversity of shifting IOD and El Niño dominates the location of Maritime Continent autumn drought. *National Science Review*, 7(7):1150–1153.
- Hudson, J. and Maloney, E. (2023). The Role of Surface Fluxes in MJO Propagation through the Maritime Continent. *Journal of Climate*, 36(6):1633–1652.
- Hutchings, J. A. and Konecky, B. L. (2023). Optimization of a Picarro L2140-i cavity ring-down spectrometer for routine measurement of triple oxygen isotope ratios in meteoric waters. *Atmospheric Measurement Techniques*, 16(6):1663–1682.
- Jackisch, D., Yeo, B. X., Switzer, A. D., He, S., Cantarero, D. L. M., Siringan, F. P., and Goodkin, N. F. (2022). Precipitation stable isotopic signatures of tropical cyclones in Metropolitan Manila, Philippines, show significant negative isotopic excursions. *Natural Hazards and Earth System Sciences*, 22(1):213–226.
- Jones, G. L. and Qin, Q. (2022). Markov chain Monte Carlo in practice. *Annual Review of Statistics and Its Application*, 9:557–578.
- Kang, X., Niu, Y., Yu, H., Gou, P., Hou, Q., Lu, X., and Wu, Y. (2022). Effect of rainfall-runoff process on sources and transformations of nitrate using a combined approach of dual isotopes, hydrochemical and Bayesian model in the Dagang River basin. *Science of the Total Environment*, 837:155674.
- Karras, C., Karras, A., Avlonitis, M., and Sioutas, S. (2022). An overview of mcmc methods: From theory to applications. In *IFIP International Conference on Artificial Intelligence Applications and Innovations*, pages 319–332. Springer.
- Klauenberg, K., Wübbeler, G., Mickan, B., Harris, P., and Elster, C. (2015). A tutorial on Bayesian normal linear regression. *Metrologia*, 52(6):878.

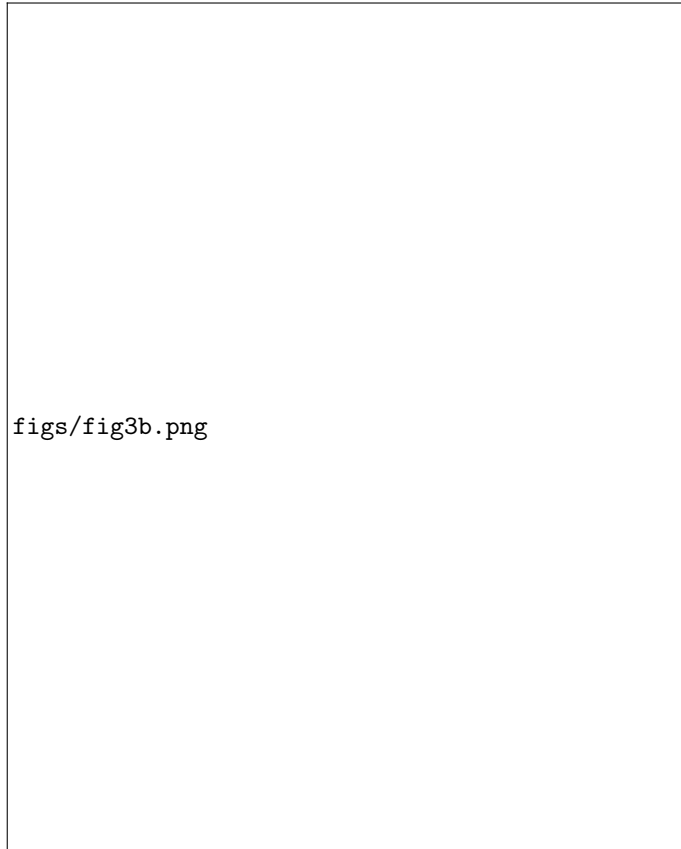
- Kurita, N., Ichiyanagi, K., Matsumoto, J., Yamanaka, M. D., and Ohata, T. (2009). The relationship between the isotopic content of precipitation and the precipitation amount in tropical regions. *Journal of Geochemical Exploration*, 102(3):113–122.
- Li, M., Gordon, A. L., Gruenburg, L. K., Wei, J., and Yang, S. (2020). Interannual to decadal response of the Indonesian throughflow vertical profile to Indo-Pacific forcing. *Geophysical Research Letters*, 47(11):e2020GL087679.
- Liu, J. Y., Zhang, F. P., Feng, Q., Wei, Y. F., Huang, L. H., Li, Z. X., Nie, S., and Li, L. (2019). Stable isotopes characteristics of precipitation over Shaanxi-Gansu-Ningxia and its water vapor sources. *The Journal of Applied Ecology*, 30(7):2191–2200.
- Lu, J., Li, T., and Shen, X. (2023). Precipitation diurnal cycle over the maritime continent modulated by ENSO. *Climate Dynamics*, 61:2547–2564.
- Maithani, S. and Pradhan, M. (2020). Cavity ring-down spectroscopy and its applications to environmental, chemical and biomedical systems. *Journal of Chemical Sciences*, 132:1–19.
- Makarim, S., Sprintall, J., Liu, Z., Yu, W., Santoso, A., Yan, X.-H., and Susanto, R. D. (2019). Previously unidentified Indonesian Throughflow pathways and freshening in the Indian Ocean during recent decades. *Scientific Reports*, 9(1):7364.
- Malik, F., Butt, S., and Mujahid, N. (2022). Variation in isotopic composition of precipitation with identification of vapor source using deuterium excess as tool. *Journal of Radioanalytical and Nuclear Chemistry*, pages 1–8.
- Mao, H., Wang, C., Qu, S., Liao, F., Wang, G., and Shi, Z. (2023). Source and evolution of sulfate in the multi-layer groundwater system in an abandoned mine—Insight from stable isotopes and Bayesian isotope mixing model. *Science of the Total Environment*, 859:160368.
- Mäs, S., Henzen, D., Bernard, L., Müller, M., Jirka, S., and Senner, I. (2018). Generic schema descriptions for comma-separated values files of environmental data. In *The 21th AGILE International Conference on Geographic Information Science*.
- McKinney, W. et al. (2011). pandas: a foundational Python library for data analysis and statistics. *Python for high performance and scientific computing*, 14(9):1–9.
- Merlivat, L. and Jouzel, J. (1979). Global climatic interpretation of the deuterium-oxygen 18 relationship for precipitation. *Journal of Geophysical Research: Oceans*, 84(C8):5029–5033.
- Metropolis, N., Rosenbluth, A. W., Rosenbluth, M. N., Teller, A. H., and Teller, E. (1953). Equation of state calculations by fast computing machines. *The Journal of Chemical Physics*, 21(6):1087–1092.
- Munksgaard, N. C., Kurita, N., Sánchez-Murillo, R., Ahmed, N., Araguas, L., Balachew, D. L., Bird, M. I., Chakraborty, S., Chinh, N. K., Cobb, K. M., et al. (2019). Data descriptor: Daily observations of stable isotope ratios of rainfall in the tropics. *Scientific Reports*, 9(1):14419.
- Nagai, T., Hibiya, T., and Syamsudin, F. (2021). Direct estimates of turbulent mixing in the Indonesian archipelago and its role in the transformation of the Indonesian throughflow waters. *Geophysical Research Letters*, 48(6):e2020GL091731.
- Nan, Y., He, Z., Tian, F., Wei, Z., and Tian, L. (2021). Can we use precipitation isotope outputs of isotopic general circulation models to improve hydrological modeling in large mountainous catchments on the Tibetan Plateau? *Hydrology and Earth System Sciences*, 25(12):6151–6172.
- Peatman, S. C., Schwendike, J., Birch, C. E., Marsham, J. H., Matthews, A. J., and Yang, G.-Y. (2021). A local-to-large scale view of Maritime Continent rainfall: Control by ENSO, MJO, and equatorial waves. *Journal of Climate*, 34(22):8933–8953.
- Peng, P., Zhang, X. J., and Chen, J. (2020). Bias correcting isotope-equipped GCMs outputs to build precipitation oxygen isoscape for eastern China. *Journal of Hydrology*, 589:125153.
- Perkel, J. (2016). Democratic databases: science on GitHub. *Nature*, 538(7623):127–128.
- Pfahl, S. and Sodemann, H. (2014). What controls deuterium excess in global precipitation? *Climate of the Past*, 10(2):771–781.

- Putman, A. L., Fiorella, R. P., Bowen, G. J., and Cai, Z. (2019). A global perspective on local meteoric water lines: Meta-analytic insight into fundamental controls and practical constraints. *Water Resources Research*, 55(8):6896–6910.
- Routson, C. C., McKay, N. P., Kaufman, D. S., Erb, M. P., Goosse, H., Shuman, B. N., Rodysill, J. R., and Ault, T. (2019). Mid-latitude net precipitation decreased with Arctic warming during the Holocene. *Nature*, 568(7750):83–87.
- Rozanski, K., Araguás-Araguás, L., and Gonfiantini, R. (1993). Isotopic patterns in modern global precipitation. *Climate change in continental isotopic records*, 78:1–36.
- Sagayama, H., Racine, N. M., Shriver, T. C., and Schoeller, D. A. (2021). Comparison of isotope ratio mass spectrometry and cavity ring-down spectroscopy procedures and precision of the doubly labeled water method in different physiological specimens. *Rapid Communications in Mass Spectrometry*, 35(21):e9188.
- Salvatier, J., Wiecki, T. V., and Fonnesbeck, C. (2016). Probabilistic programming in Python using PyMC3. *PeerJ Computer Science*, 2:e55.
- Sánchez-Murillo, R., Durán-Quesada, A. M., Birkel, C., Esquivel-Hernández, G., and Boll, J. (2017). Tropical precipitation anomalies and d-excess evolution during El Niño 2014-16. *Hydrological Processes*, 31(4):956–967.
- Santoso, A., England, M. H., Kajtar, J. B., and Cai, W. (2022). Indonesian Throughflow Variability and Linkage to ENSO and IOD in an Ensemble of CMIP5 Models. *Journal of Climate*, 35(10):3161–3178.
- Shao, L., Tian, L., Cai, Z., Wang, C., and Li, Y. (2021). Large-scale atmospheric circulation influences the ice core d-excess record from the central Tibetan Plateau. *Climate Dynamics*, 57(7-8):1805–1816.
- Sharma, S. and Mujumdar, P. P. (2022). Modeling concurrent hydroclimatic extremes with parametric multivariate extreme value models. *Water Resources Research*, 58(2):e2021WR031519.
- South, L. F., Riabiz, M., Teymur, O., and Oates, C. J. (2022). Postprocessing of MCMC. *Annual Review of Statistics and Its Application*, 9:529–555.
- Supari, Tangang, F., Salimun, E., Aldrian, E., Sopaheluwakan, A., and Juneng, L. (2018). ENSO modulation of seasonal rainfall and extremes in Indonesia. *Climate Dynamics*, 51:2559–2580.
- Suwarman, R., Ichiyanagi, K., Tanoue, M., Yoshimura, K., Mori, S., Yamanaka, M. D., Kurita, N., and Syamsudin, F. (2013). The variability of stable isotopes and water origin of precipitation over the Maritime Continent. *SOLA*, 9:74–78.
- Suwarman, R., Ichiyanagi, K., Tanoue, M., Yoshimura, K., Mori, S., Yamanaka, M. D., Syamsudin, F., and Belgaman, H. A. (2017). El niño southern oscillation signature in atmospheric water isotopes over maritime continent during wet season. *Journal of the Meteorological Society of Japan. Ser. II*, 95(1):49–66.
- Taylor, D. (2015). Work the shell: analyzing comma-separated values (csv) files. *Linux Journal*, 2015(260):3.
- Torres-Martínez, J. A., Mora, A., Knappett, P. S. K., Ornelas-Soto, N., and Mahlknecht, J. (2020). Tracking nitrate and sulfate sources in groundwater of an urbanized valley using a multi-tracer approach combined with a bayesian isotope mixing model. *Water Research*, 182:115962.
- Tritschler, F., Binder, M., Händel, F., Burghardt, D., Dietrich, P., and Liedl, R. (2020). Collected Rain Water as Cost-Efficient Source for Aquifer Tracer Testing. *Groundwater*, 58(1):125–131.
- Uieda, L., Tian, D., Leong, W. J., Schlitzer, W., Grund, M., Jones, M., Fröhlich, Y., Toney, L., Yao, J., Magen, Y., Tong, J.-H., Materna, K., Belem, A., Newton, T., Anant, A., Ziebarth, M., Quinn, J., and Wessel, P. (2023). PyGMT: A Python interface for the Generic Mapping Tools. Software available from <https://doi.org/10.5281/zenodo.7772533>.
- Valdivielso, S., Vázquez-Suñé, E., and Custodio, E. (2020). Origin and variability of oxygen and hydrogen isotopic composition of precipitation in the Central Andes: A review. *Journal of Hydrology*, 587:124899.
- Van Der Walt, S., Colbert, S. C., and Varoquaux, G. (2011). The NumPy array: a structure for efficient numerical computation. *Computing in science & engineering*, 13(2):22–30.
- Vinnarasí, R. and Dhanya, C. T. (2022). Time-varying Intensity-Duration-Frequency relationship through climate-informed covariates. *Journal of Hydrology*, 604:127178.

- Wei, Y., Pu, Z., and Zhang, C. (2020). Diurnal cycle of precipitation over the Maritime Continent under modulation of MJO: Perspectives from cloud-permitting scale simulations. *Journal of Geophysical Research: Atmospheres*, 125(13):e2020JD032529.
- Wessel, P., Luis, J. F., Uieda, L., Scharroo, R., Wobbe, F., Smith, W. H. F., and Tian, D. (2019). The Generic Mapping Tools Version 6. *Geochemistry, Geophysics, Geosystems*, 20(11):5556–5564.
- West, M. (1984). Outlier models and prior distributions in Bayesian linear regression. *Journal of the Royal Statistical Society Series B: Statistical Methodology*, 46(3):431–439.
- Xia, C., Liu, G., Chen, K., Hu, Y., Zhou, J., Liu, Y., and Mei, J. (2020). Stable isotope characteristics for precipitation events and their responses to moisture and environmental changes during the summer monsoon period in southwestern china. *Polish Journal of Environmental Studies*, 29(3).
- Xia, C., Liu, G., Mei, J., Meng, Y., Liu, W., and Hu, Y. (2019a). Characteristics of hydrogen and oxygen stable isotopes in precipitation and the environmental controls in tropical monsoon climatic zone. *International Journal of Hydrogen Energy*, 44(11):5417–5427.
- Xia, C. C., Chen, K., Zhou, J., Mei, J., Liu, Y. P., and Liu, G. D. (2019b). Comparison of precipitation stable isotopes during wet and dry seasons in a subtropical monsoon climate region of China. *Applied Ecology & Environmental Research*, 17(5).
- Xiao, H.-M., Lo, M.-H., and Yu, J.-Y. (2022). The increased frequency of combined El Niño and positive IOD events since 1965s and its impacts on maritime continent hydroclimates. *Scientific Reports*, 12(1):7532.
- Xu, H., Song, S., Guo, T., and Wang, H. (2022). Two-stage hybrid model for hydrological series prediction based on a new method of partitioning datasets. *Journal of Hydrology*, 612:128122.
- Xue, P., Malanotte-Rizzoli, P., Wei, J., and Eltahir, E. A. B. (2020). Coupled ocean-atmosphere modeling over the Maritime Continent: A review. *Journal of Geophysical Research: Oceans*, 125(6):e2019JC014978.
- Yamanaka, M. D. (2016). Physical climatology of Indonesian maritime continent: An outline to comprehend observational studies. *Atmospheric Research*, 178:231–259.
- Yang, S., Zhang, T., Li, Z., and Dong, S. (2019). Climate variability over the maritime continent and its role in global climate variation: A review. *Journal of Meteorological Research*, 33(6):993–1015.
- Yoshikawa, K., Úbeda, J., Masías, P., Pari, W., Apaza, F., Vasquez, P., Ccallata, B., Concha, R., Luna, G., Iparaguirre, J., et al. (2020). Current thermal state of permafrost in the southern Peruvian Andes and potential impact from El Niño–Southern Oscillation (ENSO). *Permafrost and Periglacial Processes*, 31(4):598–609.
- Zaryab, A., Nassery, H. R., Knoeller, K., Alijani, F., and Minet, E. (2022). Determining nitrate pollution sources in the Kabul Plain aquifer (Afghanistan) using stable isotopes and Bayesian stable isotope mixing model. *Science of the Total Environment*, 823:153749.
- Zhang, J. and Xu, Z. (2023). Vacuum extraction of high-salinity water for the determination of oxygen and hydrogen isotopic compositions using cavity ring-down spectroscopy. *Microchemical Journal*, 190:108678.
- Zhang, Q., Wang, H., and Lu, C. (2020). Tracing sulfate origin and transformation in an area with multiple sources of pollution in northern China by using environmental isotopes and Bayesian isotope mixing model. *Environmental Pollution*, 265:115105.
- Zhu, J., Guan, Z., and Wang, X. (2022). Variations of Summertime SSTA Independent of ENSO in the Maritime Continent and Their Possible Impacts on Rainfall in the Asian–Australian Monsoon Region. *Journal of Climate*, 35(24):7949–7964.
- Zolghadr-Asli, B., Bozorg-Haddad, O., Enayati, M., and Loáiciga, H. A. (2022). Sensitivity of non-conditional climatic variables to climate-change deep uncertainty using Markov Chain Monte Carlo simulation. *Scientific Reports*, 12(1):1813.



(a)

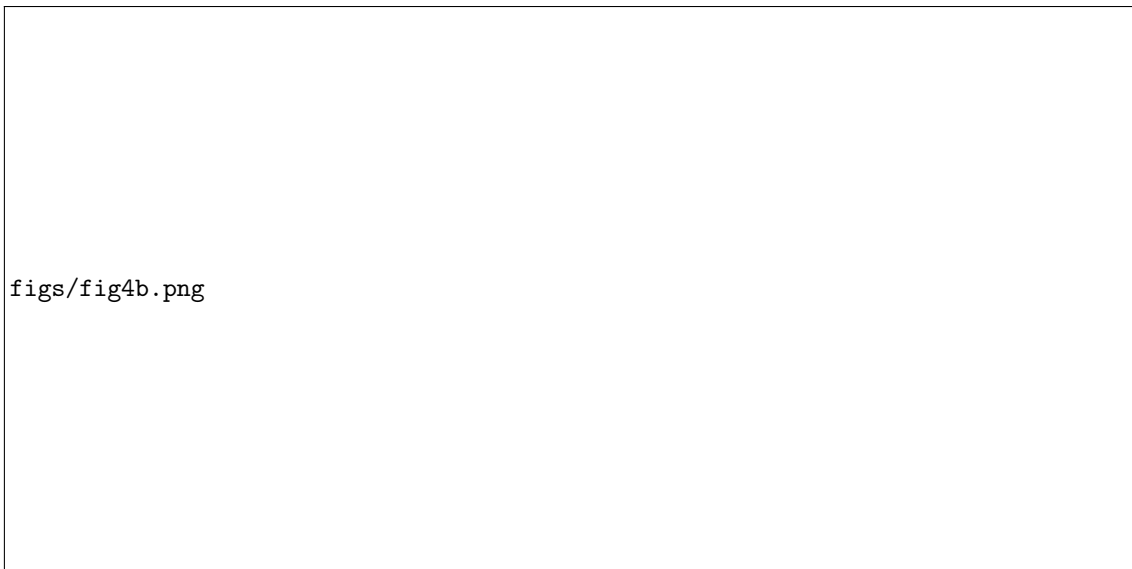


(b)

Figure 3: Box plots of the monthly (a) $\delta^{18}\text{O}$ and (b) $\delta^2\text{H}$ recorded by the 62 stations between September 2010 and September 2017.



(a)



(b)

Figure 4: (a) BLR posterior parameter trace plots for the intercept (upper panel), slope (middle panel), and standard deviation (lower panel). (b) Posterior distribution of the three linear regression parameters: intercept (upper panel), slope (middle panel), and standard deviation (lower panel).

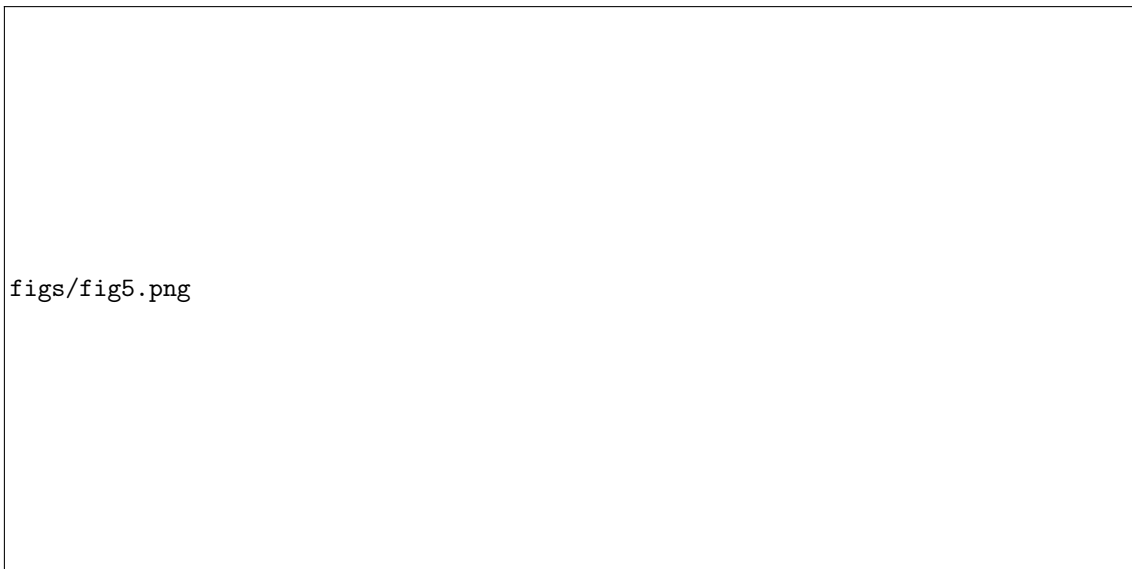


Figure 5: The GMWL (solid black line) compared to the LMWL (the posterior mean shown by a solid red line, area between the dashed red lines shows 95% credible interval obtained from the highest posterior density interval (HPDI)) of all stations over the IMC. Grey dots indicate individual data points.